

# Photo-heating and the fate of hard photons during the reionisation of He II by quasars

James S. Bolton<sup>1</sup>, S. Peng Oh<sup>2</sup> & Steven R. Furlanetto<sup>3</sup>

<sup>1</sup> *Max Planck Institut für Astrophysik, Karl-Schwarzschild Str. 1, 85748 Garching, Germany*

<sup>2</sup> *Department of Physics, University of California, Santa Barbara, CA 93106, USA*

<sup>3</sup> *Department of Physics and Astronomy, University of California, Los Angeles, CA 90095, USA*

17 March 2009

## ABSTRACT

We use a combination of analytic and numerical arguments to consider the impact of quasar photo-heating during He II reionisation on the thermal evolution of the intergalactic medium (IGM). We demonstrate that rapid ( $\Delta z < 0.1\text{--}0.2$ ), strong ( $\Delta T > 10^4$  K) photo-heating is difficult to achieve across the entire IGM unless quasar spectra are significantly harder than implied by current observational constraints. Although filtering of intrinsic quasar radiation through dense regions in the IGM does increase the mean excess energy per He II photo-ionisation, it also weakens the radiation intensity and lowers the photo-ionisation rate, preventing rapid heating over time intervals shorter than the local photo-ionisation timescale. Moreover, the hard photons responsible for the strongest heating are more likely to deposit their energy inside dense clumps, which cool rapidly and are furthermore invisible to most observational probes of the IGM temperature. The abundance of such clumps is, however, uncertain and model-dependent, leading to a fairly large uncertainty in the photo-heating rates. Nevertheless, although some of the IGM may be exposed to a hardened and weakened ionising background for long periods, most of the IGM must instead be reionised by the more abundant, softer photons and with accordingly modest heating rates ( $\Delta T \lesssim 10^4$  K), although localised patches of much higher temperature are still possible. The repeated ionisation of fossil quasar He III regions does not increase the net heating because the recombination times in these regions typically exceed the IGM cooling times and the average time lag between successive rounds of quasar activity. Detailed line-of-sight radiative transfer simulations confirm these expectations and predict a rich thermal structure in the IGM during He II reionisation. The resulting complex relationship between temperature and density may help resolve discrepancies between optically thin simulations of the Ly $\alpha$  forest and recent observations.

**Key words:** radiative transfer - methods: numerical - intergalactic medium - quasars: absorption lines - cosmology:theory.

## 1 INTRODUCTION

Helium, the second most abundant chemical element in the Universe, is expected to be singly ionised at the same time as hydrogen due to its similar ionisation potential (24.6 eV), larger photo-ionisation cross-section and lower abundance relative to hydrogen. Even for ionising sources with relatively soft, stellar like spectra, the reionisation of H I and He I in the IGM is expected to be concurrent (*e.g.* Giroux & Shapiro 1996). In contrast, the much larger ionisation threshold (54.4 eV) and smaller photo-ionisation cross-section of singly ionised helium requires that He II reionisation proceeds only when sources

with sufficiently hard spectra become numerous. A putative population of massive, metal free stars (Oh et al. 2001; Venkatesan et al. 2003), high redshift X-rays (Oh 2001; Venkatesan et al. 2001; Ricotti & Ostriker 2004) or thermal emission from shock heated gas (Miniati et al. 2004) may provide the requisite ionising photons. The stacked spectra of Lyman break galaxies at  $z \sim 3$  (Shapley et al. 2003) also exhibit an He II recombination line strong enough to suggest that galaxies may contribute significantly to He II reionisation (Furlanetto & Oh 2008b). However, quasars are considered to be the most likely candidates for completing He II reionisation (Madau et al.

1999; Miralda-Escudé et al. 2000; Sokasian et al. 2002; Bolton et al. 2006; Furlanetto & Oh 2008b; Paschos et al. 2007), although bright quasars are rare at high redshift and unlikely to contribute substantially to either the H I or He II ionising photon budget at  $z > 5$  (Dijkstra et al. 2004; Meiksin 2005; Sribinovsky & Wyithe 2007; Bolton & Haehnelt 2007b; Jiang et al. 2008). Consequently, unless He II reionisation was completed by an as yet unidentified population of sources with hard spectra at  $z > 5$ , its latter stages are expected to coincide with the observed peak in quasar activity around  $z \simeq 2 - 3$ .

There are several pieces of observational evidence which may support this picture. Observations of the He II Ly $\alpha$  Gunn-Peterson trough and patchy absorption in the He II Ly $\alpha$  forest at  $z \simeq 3$  indicate a situation analogous to that implied by the H I opacity data at  $z \simeq 6$  (Jakobsen et al. 1994; Davidsen et al. 1996; Heap et al. 2000; Smette et al. 2002; Zheng et al. 2004; Shull et al. 2004; Reimers et al. 2005; Fechner et al. 2006). However, like the H I measurements at higher redshift (*e.g.* Fan et al. 2006; Becker et al. 2007), the interpretation of the He II data is hampered by its insensitivity to the He II fraction once the Ly $\alpha$  absorption becomes saturated. Other indirect evidence includes an apparent boost to the IGM temperature at  $z \simeq 3.3$  (Schaye et al. 2000; Ricotti et al. 2000), measurements of metal line ratios which indicate the ultraviolet (UV) background is hardening around the same redshifts (Songaila 1998; Vladilo et al. 2003), and the detection of a sharp dip in the H I Ly $\alpha$  forest effective optical depth at  $z \simeq 3.2$  (Bernardi et al. 2003; Faucher-Giguere et al. 2008). The latter result may be associated with the observed boost in the IGM temperature at the same redshifts (Theuns et al. 2002a). On the other hand, conflicting evidence exists for all of these cases (*e.g.* Zaldarriaga et al. 2001; Kim et al. 2002; McDonald et al. 2001, 2005). Thus, the observational evidence for He II reionisation remains controversial.

Nevertheless, from a theoretical standpoint it is still expected He II reionisation will have a significant impact on the thermal state of the IGM (Miralda-Escudé & Rees 1994; Abel & Haehnelt 1999; Theuns et al. 2002a; Paschos et al. 2007; Furlanetto & Oh 2008a). Firstly, energy injected by the hard sources which reionise He II will raise the IGM temperature. This is consistent with some of the observational constraints derived from Ly $\alpha$  forest line widths which imply a boost of  $\Delta T \simeq 1-2 \times 10^4$  K around  $z \sim 3$  (Schaye et al. 2000; Ricotti et al. 2000). The magnitude of the increase will depend on the spectrum of the intrinsic ionising radiation, and thus also on the amount it is subsequently filtered by the intervening IGM (Abel & Haehnelt 1999). Secondly, the reionisation of He II will alter the temperature-density relation of the IGM. In the optically thin limit, the IGM will follow a tight polytropic temperature-density relation,  $T = T_0 \Delta^{\gamma-1}$ , expected to arise for normalised densities  $\Delta = \rho/\langle\rho\rangle \leq 10$  when photo-heating by a spatially uniform UV background is balanced by cooling due to adiabatic expansion (Hui & Gnedin 1997; Valageas et al. 2002). However, the assumption of a spatially uniform UV background ionising an optically thin IGM will break down during He II reionisation. Instead, radiative transfer effects and/or the inhomogeneous distribution of the ionising sources will produce a complex, multi-

valued and perhaps even inverted ( $\gamma < 1$ ) temperature-density relation (Gleser et al. 2005; Tittley & Meiksin 2007; Furlanetto & Oh 2008a; Bolton et al. 2008).

Despite all of these studies, very little work has been done to establish a physical argument for exactly how large the temperature boost in the IGM during He II reionisation will be. Furthermore, it is unclear over what timescale any global temperature boost should occur. This depends on understanding how photo-heating in an optically thick IGM proceeds, and thus on the details of radiative transfer through the inhomogeneous IGM. The observational evidence provides valuable hints, but the data are still too poorly constrained to distinguish between different models in detail. A wide variety of values for the temperature boost during He II reionisation,  $5\,000\text{ K} < \Delta T < 30\,000\text{ K}$ , have therefore been adopted in the literature, with the timescales for the temperature boost varying from instantaneous to periods spanning several redshift units (*e.g.* Abel & Haehnelt 1999; Theuns et al. 2002a; Inoue & Kamaya 2003; Hui & Haiman 2003; Furlanetto & Oh 2008a). The main reason for this is that photo-heating in an optically thick IGM during He II reionisation is almost always modelled in an approximate way. Only a handful of studies have explicitly quantified the expected IGM temperature boost during He II reionisation using radiative transfer calculations. Abel & Haehnelt (1999) were the first to point out the importance of radiative transfer through an optically thick IGM. Using one dimensional radiative transfer simulations, they found the filtering of ionising radiation through the IGM could increase He II photo-heating rates by a factor of 1.5–2.5 above the optically thin values, leading to  $\Delta T \sim 10^4$  K. More recently, Tittley & Meiksin (2007) demonstrated that the temperature boost depends sensitively on the typical spectra of the sources which drive He II reionisation. Finally, Paschos et al. (2007) have presented a detailed, three dimensional radiative transfer simulation of He II reionisation. They found that radiative transfer effects could boost the IGM temperature by around a factor of two. However, none of these studies explicitly discuss over what timescale this heat input may reasonably occur, or how the temperature boost depends in detail on the density distribution of the intervening IGM.

A clear understanding of photo-heating during He II reionisation is thus vital for interpreting the thermal history of the IGM. In this paper we critically re-examine the photo-heating of the IGM by quasars during He II reionisation. In particular, using a combination of analytical arguments and line-of-sight radiative transfer calculations, we shall address what the likely temperature boost in the IGM during He II reionisation is, and how rapidly this temperature boost should occur. Furthermore, we consider what the fate of the hard photons responsible for heating the IGM is likely to be: where do they end up in the IGM, and how important is the filtering of ionising radiation through the IGM in setting the temperature during He II reionisation?

We begin in §2, where we briefly outline the relationship between He II photo-heating and the photo-ionisation timescale. This argument is key to establishing the amount of heat which may be injected into the IGM within a given time. In §3 we present a model for estimating the maximum

temperature achievable during He II reionisation in an optically thick IGM. A more detailed treatment of the filtering of He II ionising photons through a clumpy medium is presented in §4, and in §5 we consider the impact of He II photo-heating in recombining fossil He III regions. We then compare our analytical results with detailed line-of-sight radiative transfer simulations in §6, and use these results to discuss the impact of He II reionisation on the IGM temperature density relation in §7. We summarise our results, compare them to current observational constraints and conclude in §8.

Throughout this paper we shall assume  $\Omega_m = 0.26$ ,  $\Omega_\Lambda = 0.74$ ,  $\Omega_b h^2 = 0.024$ ,  $h = 0.72$ ,  $\sigma_8 = 0.85$ ,  $n_s = 0.95$  and an IGM of primordial composition with a helium mass fraction of  $Y = 0.24$  (e.g. Olive & Skillman 2004). The cosmological parameters are consistent with the most recent WMAP results (Dunkley et al. 2008) aside from a slightly larger normalisation for the power spectrum. Unless otherwise stated, all distances are expressed as comoving quantities.

## 2 ON He II PHOTO-HEATING AND THE PHOTO-IONISATION TIMESCALE

We begin by considering an ideal gas parcel of density  $\rho$  exposed to a spatially uniform ionising radiation field with specific intensity  $J_\nu = J_{-21}(\nu/\nu_{\text{HI}})^{-\alpha_s}$ , where  $J_{-21} = J_{\text{HI}}/10^{-21}$  erg s<sup>-1</sup> cm<sup>-2</sup> Hz<sup>-1</sup> sr<sup>-1</sup> and  $\nu_{\text{HI}}$  are the specific intensity and frequency at the H I ionisation threshold, respectively, and  $\alpha_s$  is a power-law spectral index. The thermal evolution of the gas parcel in a cosmologically expanding medium is then (e.g. Hui & Gnedin 1997; Furlanetto & Oh 2008a)

$$\frac{dT}{dt} = \frac{2\mu m_{\text{H}}}{3k_{\text{B}}\rho} [\mathcal{H} - \Lambda] + \frac{2T}{3(1+\delta)} \frac{d\delta}{dt} + \frac{T}{\mu} \frac{d\mu}{dt} - 2HT, \quad (1)$$

where  $\mu = [(1-Y)(1+n_e/n_{\text{H}}) + Y/4]^{-1}$  is the mean molecular weight of the gas,  $\mathcal{H} = \sum_i n_i \epsilon_i$  is the total photo-heating rate per unit volume summed over the species  $i = [\text{H I}, \text{He I}, \text{He II}]$  with number density  $n_i$ ,  $\Lambda$  is the cooling rate per unit volume,  $\delta \equiv \Delta - 1$  is the density contrast,  $H$  is the Hubble parameter and all other symbols have their usual meaning.

The first term in eq. (1) is the dominant heating term; during reionisation  $\mathcal{H} \gg \Lambda$  at the low densities and temperatures typical of most of the IGM (Efstathiou 1992; Katz et al. 1996). The photo-heating rate for species  $i = [\text{H I}, \text{He I}, \text{He II}]$  is

$$\epsilon_i = \int_{\nu_i}^{\infty} \frac{4\pi J_\nu}{h_{\text{p}}\nu} \sigma_\nu^i h_{\text{p}}(\nu - \nu_i) e^{-\tau_\nu} d\nu, \quad (2)$$

where  $\tau_\nu = \sum_j \tau_\nu^j$  is the optical depth to the ionising photons summed over the species  $j = [\text{H I}, \text{He I}, \text{He II}]$  and  $\nu_i$  is the frequency at the relevant ionisation threshold. Note here that  $J_\nu$  is an *intrinsic* spectrum and does not include any reprocessing by the IGM. The second term in eq. (1) describes the adiabatic heating or cooling due to structure formation, and is small for the modest density contrasts associated with most of the IGM. The third term, which results from changes in the mean molecular weight of the gas parcel, is also small compared to the photo-heating rate during

He II reionisation. The final term corresponds to the adiabatic cooling driven by the expansion of the Universe, and is the dominant cooling term at the moderate to low densities ( $\Delta \lesssim 10$ ) still expanding with the Hubble flow. The relevant cooling timescale for the low density, photo-ionised gas in the IGM is therefore always the Hubble time,  $t_{\text{H}}$  (Miralda-Escudé & Rees 1994).

Let us now assume the H I and He I in the gas parcel has already been ionised at some earlier time, and that the reionisation of He II is now completed by the radiation field  $J_\nu$ . We shall further assume that the gas parcel is exposed to this radiation field for a time  $t_s \ll t_{\text{H}}$ . The temperature evolution of the gas parcel at  $z \simeq 3$  may then be approximated by

$$\frac{dT}{dt} \simeq \frac{2\mu m_{\text{H}}}{3k_{\text{B}}\rho} n_{\text{HeII}} \epsilon_{\text{HeII}}. \quad (3)$$

Ignoring the collisional ionisation of He II, which is a reasonable approximation in the presence of large photo-ionisation rates, the rate of change of  $n_{\text{HeII}}$  is

$$\frac{dn_{\text{HeII}}}{dt} = n_e n_{\text{HeIII}} \alpha_{\text{HeIII}} - n_{\text{HeII}} (\Gamma_{\text{HeII}} + n_e \alpha_{\text{HeII}}), \quad (4)$$

where  $\alpha_i$  are the recombination rates for species  $i$  and in general the photo-ionisation rate for species  $i = [\text{H I}, \text{He I}, \text{He II}]$  is

$$\Gamma_i = \int_{\nu_i}^{\infty} \frac{4\pi J_\nu}{h_{\text{p}}\nu} \sigma_\nu^i e^{-\tau_\nu} d\nu. \quad (5)$$

Finally, assuming the case B He III recombination timescale  $t_{\text{rec}} \simeq 1.4 \times 10^9$  yrs  $\Delta^{-1} (T/10^4 \text{ K})^{0.7} [(1+z)/4]^{-3} \gg t_s$ , eq. (4) reduces to  $n_{\text{HeII}} \simeq \Gamma_{\text{HeII}}^{-1} |dn_{\text{HeII}}/dt|$ , and upon substitution in eq. (3) yields

$$\frac{dT}{dt} \simeq \frac{2\mu m_{\text{H}}}{3k_{\text{B}}\rho} \left| \frac{dn_{\text{HeII}}}{dt} \right| \langle E \rangle_{\text{HeII}}, \quad (6)$$

where  $\langle E \rangle_{\text{HeII}} = \epsilon_{\text{HeII}}/\Gamma_{\text{HeII}}$  is the mean excess energy per He II photo-ionisation. In the optically thin limit ( $\tau_\nu \ll 1$ ) and assuming the photo-ionisation cross-sections are proportional to  $\nu^{-3}$ , this reduces to  $\langle E \rangle_{\text{HeII}} \simeq h_{\text{p}} \nu_{\text{HeII}} / (\alpha_s + 2)$  (Abel & Haehnelt 1999). Eq. (6) thus elucidates the key parameters which influence the temperature of an optically thin gas parcel during He II reionisation;  $\langle E \rangle_{\text{HeII}} = \epsilon_{\text{HeII}}/\Gamma_{\text{HeII}}$ , which depends *only* on the spectral shape and not the specific intensity of the ionising radiation, and the rate of change of  $n_{\text{HeII}}$ , which *does* implicitly depend on the intensity<sup>1</sup>. Expressed differently,  $|dn_{\text{HeII}}/dt| \simeq n_{\text{HeII}}/t_{\text{ion}}$ , where  $t_{\text{ion}} = \Gamma_{\text{HeII}}^{-1}$  is the He II photo-ionisation timescale. If  $t_{\text{ion}} \gg t_s$ , no significant heating will occur in the gas parcel irrespective of the average excess energy per photo-ionisation.<sup>2</sup>

<sup>1</sup> In the optically thick case the ionising radiation will be hardened and weakened by the intervening gas, but the general result remains the same. We assume the gas parcel is optically thin in this instance for simplicity.

<sup>2</sup> On longer timescales ( $\gg t_{\text{ion}}$ ) ionisation equilibrium is achieved and recombinations become important. Then in general for a species  $i$ ,  $dT/dt \propto \rho \alpha_i \langle E \rangle_{\text{HeII}}$  (e.g. Theuns 2005). The heating rate is now proportional to the IGM density and is independent of the intensity of the ionising radiation if the ionised fraction is close to unity.

Although this argument is applied here to a single optically thin gas parcel for simplicity, it also extends more generally to the IGM as a whole. A substantial temperature boost in the IGM can only occur globally within a timescale  $t_s$  if the He II ionising background is sufficiently hard *and* intense. If the condition  $t_{\text{ion}} < t_s$  is not met everywhere, the He II ionisation rate is too low to significantly photo-heat the entire IGM. Instead, temperature boosts are possible only in the vicinity of quasars where the local He II photo-ionisation rate is large. Alternatively, a large, global IGM temperature boost over longer timescales is still possible if the He II ionising background is weak, yet hard and persistent. Crucially, these scenarios depend on exactly how many hard photons are produced by quasars over time and the impact of the subsequent transfer of radiation through the IGM on the intrinsic quasar emission. Bearing these points in mind, we now proceed to discuss the expected temperature of the IGM during He II reionisation in more detail.

### 3 THE TEMPERATURE IN AN OPTICALLY THICK IGM DURING He II REIONISATION

#### 3.1 Radiative transfer and the IGM temperature

The temperature boost in the IGM during He II reionisation is approximately (Furlanetto & Oh 2008a)

$$\Delta T \simeq 0.035 f_{\text{HeII}} \left( \frac{2}{3k_B} \right) \langle E \rangle_{\text{HeII}}, \quad (7)$$

where  $f_{\text{HeII}} = n_{\text{HeII}}/n_{\text{He}}$  is the He II fraction in the IGM when He II photo-heating commences. This assumes the excess energy per He II photo-ionisation is shared equally among all the baryons in the IGM through Coulomb interactions. In the optically thin limit,  $\langle E \rangle_{\text{HeII}} \simeq h_p \nu_{\text{HeII}} / (\alpha_s + 2) = 15.5 \text{ eV}$  for  $\alpha_s = 1.5$ , giving  $\Delta T \simeq 4200 \text{ K}$ .

Radiative transfer effects during He II reionisation can substantially increase this temperature boost. An optically thick IGM will alter the spectral shape of any incident ionising radiation (Haardt & Madau 1996). In a uniform medium the ionising photon mean free path  $\lambda_\nu \propto \nu^3$ ; high energy ionising photons have a strongly suppressed photo-ionisation cross-section, where  $\sigma_\nu \propto \nu^{-3}$ . In an optically thick IGM the average excess energy per He II photo-ionisation is therefore progressively larger the further from the He II ionising source (Abel & Haehnelt 1999; Bolton et al. 2004). This hardened, filtered ionising radiation can then impart a significant temperature boost to the IGM compared to the optically thin case. In the optically thick limit, where every He II ionising photon is eventually absorbed and one may ignore the  $\nu^{-3}$  weighting from the photo-ionisation cross-section,  $\langle E \rangle_{\text{HeII}} \simeq h_p \nu_{\text{HeII}} / (\alpha_s - 1) = 108.8 \text{ eV}$  for  $\alpha_s = 1.5$ , leading to  $\Delta T \simeq 30\,000 \text{ K}$ . Thus, a conventional interpretation is that any large, global boost to the IGM temperature at  $z \simeq 3$  (inferred either directly or indirectly from observations) may be due to photo-heating rates which are amplified by radiative transfer effects during He II reionisation (*e.g.* Schaye et al. 2000; Ricotti et al. 2000; Theuns et al. 2002a; Bernardi et al. 2003; Faucher-Giguere et al. 2008).

Recall, however, that irrespective of how large  $\langle E \rangle_{\text{HeII}}$  is, no significant photo-heating will occur in a patch of the IGM over timescales shorter than the local photo-ionisation timescale,  $t_{\text{ion}} = \Gamma_{\text{HeII}}^{-1}$ . Ionising radiation is significantly

weakened as well as hardened at progressively larger distances from an ionising source. This clearly has implications for the  $\Delta T$  attainable over a fixed timescale. The hardest, most highly filtered radiation may be too weak to significantly heat a patch of the IGM over the short timescales associated with quasar activity. Quantifying the effect of this filtering and weakening of the ionising radiation field on the IGM temperature evolution is non-trivial; the temperature will depend on the density distribution of the intervening IGM, the intrinsic spectra and luminosities of the ionising sources, their spatial distribution and their lifetimes. Detailed numerical simulations of radiative transfer are therefore required to fully address this issue. We may nevertheless develop some intuition by first using a simple toy model for the effect of radiative transfer on the IGM temperature.

#### 3.2 A simple model for estimating ionisation timescales and temperature boosts in an optically thick IGM

Consider a quasar which emits  $\dot{N}$  ionising photons per second above the He II ionisation threshold where

$$\dot{N} = \int_{\nu_{\text{HeII}}}^{\infty} \frac{L_\nu}{h_p \nu} d\nu, \quad (8)$$

and which has a broken power law spectrum given by (*e.g.* Madau et al. 1999)

$$L_\nu \propto \begin{cases} \nu^{-0.3} & (2500 < \lambda < 4600 \text{ \AA}), \\ \nu^{-0.8} & (1050 < \lambda < 2500 \text{ \AA}), \\ \nu^{-\alpha_s} & (\lambda < 1050 \text{ \AA}). \end{cases} \quad (9)$$

There are a wide range of values for the extreme UV (EUV) spectral index,  $\alpha_s$ , observed in the quasar population at  $z > 0.33$  (Telfer et al. 2002). We adopt a fiducial value of  $\alpha_s = 1.5$ , consistent with the mean Telfer et al. (2002) obtain for radio-quiet quasars. However, the EUV spectral index is a significant uncertainty. For example, Zheng et al. (1997) find a somewhat softer mean EUV index of  $\alpha_s = 1.8$  may be appropriate, while on the other hand Scott et al. (2004) find  $\alpha_s \simeq 0.5$  at  $z < 1$ . We therefore also consider softer and harder quasar spectra with  $\alpha_s = 2.5$  and  $\alpha_s = 0.5$ , broadly consistent with the dispersion in  $\alpha_s$  measured by Telfer et al. (2002).

The rate at which He II ionising photons are produced by such a quasar with B-band luminosity  $L_B$  (where  $L_B = \nu L_\nu$  evaluated at 4400 Å) is then

$$\dot{N} \simeq 3.6 \times 10^{56} \text{ s}^{-1} \alpha_s^{-1} \left( \frac{228 \text{ \AA}}{1050 \text{ \AA}} \right)^{\alpha_s} \left( \frac{L_B}{10^{12} L_\odot} \right). \quad (10)$$

An  $L_B \simeq L_* \simeq 10^{12} L_\odot$  quasar at  $z \simeq 3$  yields  $\dot{N} = (3.3 \times 10^{56}, 2.4 \times 10^{55}, 3.1 \times 10^{54}) \text{ s}^{-1}$  for  $\alpha_s = (0.5, 1.5, 2.5)$ . Note the quasar spectrum which is harder/softer than the fiducial  $\alpha_s = 1.5$  model also emits many more/less ionising photons below the He II ionisation threshold for fixed  $L_B$ . Quasars with  $L_B \geq L_*$  are expected to dominate the He II ionising emissivity at  $z \simeq 3$  (Hopkins et al. 2007; Furlanetto & Oh 2008b). We adopt  $L_B = 10^{12} L_\odot$  as the fiducial luminosity throughout this paper.

Let us now invoke a cut-off at some arbitrary frequency in the quasar spectrum above the He II ionisation threshold,

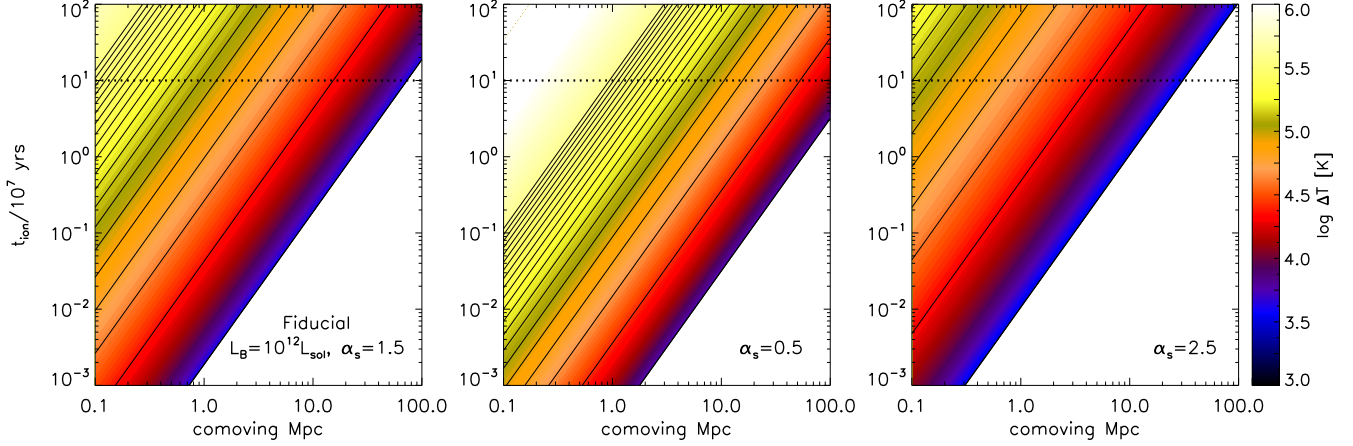


**Figure 1.** A simple model for estimating the He II photo-ionisation timescale and hence the maximum temperature boost around a single quasar for an arbitrary amount of filtering of the intrinsic quasar spectrum above the He II ionisation threshold at  $z = 3$  (see text for details). The solid black lines in each panel correspond to the ionisation timescale assuming a cut-off in the intrinsic quasar spectrum at  $\nu' = n\nu_{\text{HeII}}$ , where  $n = 1, 2, \dots, 20$ , such that the IGM is optically thin to He II ionising photons with  $\nu \geq \nu'$  only. The horizontal dotted line in each panel denotes our fiducial model quasar lifetime of  $10^8$  yrs, while the underlying colour scale shows the logarithm of the expected IGM temperature increase given by eq. (14) for the assumed cut-off frequency. The results for the fiducial quasar model, with  $L_B = 10^{12} L_\odot$  and  $\alpha_s$ , are displayed in the left-most panel. The remaining panels, from left to right, are as for fiducial model, but with  $\alpha_s = 0.5$  and  $\alpha_s = 2.5$ .

$\nu' \geq \nu_{\text{HeII}}$ . One may think of this as a condition which requires  $\tau_\nu \rightarrow \infty$  for  $\nu < \nu'$  and  $\tau_\nu \rightarrow 0$  for  $\nu \geq \nu'$ , so the IGM is optically thin only to photons with frequencies above the cut-off. This is obviously a simplification of the full radiative transfer problem; in reality the He II optical depth is a continuous function of frequency and the amount of attenuation will depend on the density distribution of the intervening IGM. This approach is nevertheless useful because it crudely mimics the effect of the filtering and weakening of the He II ionising radiation emitted by the quasar. The He II photo-ionisation rate at a comoving distance  $R$  from the quasar is

$$\Gamma_{\text{HeII}} = (1+z)^2 \int_{\nu'}^{\infty} \frac{L_\nu}{4\pi R^2} \frac{\sigma_\nu}{h\nu} d\nu. \quad (11)$$

It is then straightforward to integrate this expression to obtain

$$\begin{aligned} \Gamma_{\text{HeII}} &\simeq \frac{7.5 \times 10^{-13} \text{ s}^{-1}}{\alpha_s + 3} \left( \frac{\nu'}{\nu_{\text{HeII}}} \right)^{-\alpha_s - 3} \left( \frac{228 \text{ \AA}}{1050 \text{ \AA}} \right)^{\alpha_s} \\ &\times \left( \frac{L_B}{10^{12} L_\odot} \right) \left( \frac{R}{10 \text{ Mpc}} \right)^{-2} \left( \frac{1+z}{4} \right)^2. \end{aligned} \quad (12)$$

The photo-ionisation rate is thus strongly dependent on the frequency of the assumed cut-off in the ionising spectrum, where  $\Gamma_{\text{HeII}} \propto (\nu'/\nu_{\text{HeII}})^{-\alpha_s - 3}$ . On the other hand, the mean excess energy per He II ionisation increases with the cut-off frequency, such that

$$\langle E \rangle_{\text{HeII}} \simeq h\nu_{\text{HeII}} \left[ \frac{\nu'}{\nu_{\text{HeII}}} \left( \frac{\alpha_s + 3}{\alpha_s + 2} \right) - 1 \right]. \quad (13)$$

Assuming  $t_{\text{ion}} = \Gamma_{\text{HeII}}^{-1} < t_s$ , substituting into eq. (7) yields

$$\Delta T \simeq 14700 \text{ K } f_{\text{HeII}} \left[ \frac{\nu'}{\nu_{\text{HeII}}} \left( \frac{\alpha_s + 3}{\alpha_s + 2} \right) - 1 \right]. \quad (14)$$

Hence, for a quasar with a fixed luminosity and intrinsic spectral shape, we may estimate the *maximum* temperature boost which can be achieved through photo-heating of He II if the intrinsic spectrum has been filtered by some arbitrary but constant amount. Note that this simple argument does not include any information regarding the likelihood ionising radiation is filtered by the assumed amount, nor the timescale for which it remains filtered; to do so requires a detailed knowledge of the intervening IGM density distribution. Rather, this model assumes *a priori* that the quasar radiation is already filtered by the IGM as parameterised by the frequency cut-off  $\nu'$ , and remains so throughout the lifetime of the ionising source. We will return to the issue of how likely ionising radiation is filtered by a certain amount in §4.

Finally, we must also assume a fiducial lifetime for the quasar. Recent numerical studies indicate optically bright quasars have lifetimes of  $t_s \simeq 10^7$  yrs (Hopkins et al. 2005a), while a wide variety of observational data suggest quasar lifetimes vary from  $t_s \simeq 10^6 - 10^8$  yrs (Martini 2004). We adopt the upper limit of  $t_s = 10^8$  yr – which conservatively maximises the effect of photo-heating – as the fiducial lifetime, although we will discuss the effect of shorter quasar lifetimes later.

### 3.3 The maximum IGM temperature around individual quasars during He II reionisation

This toy model is illustrated in Fig. 1. The photo-ionisation timescale  $t_{\text{ion}} = \Gamma_{\text{HeII}}^{-1}$ , computed from eq. (12), is displayed as a function of  $R$  and  $\nu'$  for three different quasar models at  $z = 3$ . In all panels the black lines correspond to the ionisation timescale assuming  $\nu' = n\nu_{\text{HeII}}$ , where  $n = 1, 2, \dots, 20$ , and the horizontal dotted line denotes our fiducial model quasar lifetime of  $10^8$  yrs. The underlying colour scale shows the logarithm of the expected temperature increase calcu-

lated using eq. (14). The unshaded regions in the lower right of each panel lie below the minimum ionisation timescale corresponding to the unfiltered quasar radiation field, where  $\nu' = \nu_{\text{HeII}}$ .

The left-most panel Fig. 1 displays the photo-ionisation timescales for our fiducial quasar model ( $L_{\text{B}} = 10^{12} L_{\odot}$ ,  $\alpha_{\text{s}} = 1.5$ ). Recalling that we require  $t_{\text{ion}} < t_{\text{s}}$  for significant heating to occur, we see a temperature increase  $\Delta T \simeq 30\,000$  K ( $\log \Delta T \simeq 4.5$ ), expected in the optically thick limit where every ionising photon is absorbed so that  $\langle E \rangle_{\text{HeII}} \simeq h_{\text{p}} \nu_{\text{HeII}} / (\alpha_{\text{s}} - 1) = 108.8$  eV, is only possible very close to the quasar if  $t_{\text{s}} \leq 10^8$  yrs (or equivalently  $\Delta z \leq 0.13$  at  $z = 3$ ). Ionising radiation which has been hardened sufficiently to produce such a large temperature boost is too weak to photo-ionise the He II at  $R \gtrsim 10$  Mpc. A hard, intense ionising radiation field is in any case unlikely to be maintained in such close proximity to the quasar for long periods. As noted by Abel & Haehnelt (1999) (and see also §6), the IGM will instead quickly become optically thin to all He II ionising photons, thereby limiting the temperature boost within this region to a substantially smaller value. Over a quasar lifetime of  $10^8$  yrs, the temperature boost is restricted to  $\Delta T \lesssim 10^4$  K at  $\sim 40$  Mpc from the quasar, and even less at larger distances. Note again, however, that the exact amount of filtering will depend sensitively on the intervening density distribution of the IGM. In addition, we stress these temperatures represent the *maximum* possible values within a fixed volume around a quasar, since all photons with  $\nu < \nu'$  are neglected in eq. (14). Although these low energy photons do increase the total ionisation rate, they *decrease* the average heating. These estimates also ignore the effect of any cooling on the resulting IGM temperature.

Greater temperature boosts can be achieved out to larger distances around a quasar for either a harder intrinsic spectrum, a brighter luminosity, or both. The former increases the average excess energy per photo-ionisation, while the latter decreases the photo-ionisation timescale. The central panel in Fig. 1 shows the results for the model with  $L_{\text{B}} = 10^{12} L_{\odot}$  and  $\alpha_{\text{s}} = 0.5$ . In addition to having a harder spectrum, this quasar model produces around 14 times the number of He II ionising photons in our fiducial model. On the other hand, a softer, fainter quasar spectrum with  $L_{\text{B}} = 10^{12} L_{\odot}$  and  $\alpha_{\text{s}} = 2.5$ , as shown in the right-most panel of Fig. 1, yields much smaller temperatures for a given amount of filtering.

This simple model clearly illustrates the difficulty of attaining substantial temperature boosts over large volumes in the IGM within short timescales. For typical quasar EUV spectral indices and luminosities, except for regions in close proximity to the quasar, there are simply not enough hard photons to raise the IGM temperature substantially above the value expected in the optically thin limit. Furthermore, in this example we have assumed  $f_{\text{HeII}} = 1$  and  $t_{\text{s}} = 10^8$  yrs, which is around the upper limit for plausible quasar lifetimes (Martini 2004). If the lifetimes of optically bright quasars are significantly shorter than  $10^8$  yrs (Hopkins et al. 2005b), or if a patch of the IGM has  $f_{\text{HeII}} < 1$  as might be expected if fossil He III regions are common prior to the completion of He II reionisation (Furlanetto et al. 2008), then the temperature boost around a single quasar will be accordingly smaller. Thus, for our fiducial quasar model a boost to the IGM temperature on timescales  $\Delta z \lesssim 0.13$  ( $t_{\text{s}} \lesssim 10^8$  yrs at

$z \simeq 3$ ) in excess of  $\sim 10^4$  K appears unlikely over scales of  $R > 40$  Mpc. Given that the average separation between  $L_{*}$  quasars is  $\sim 100$  Mpc (Furlanetto & Oh 2008b), this implies that a rapid *global* IGM temperature boost in excess of  $\Delta T \simeq 10^4$  K is difficult to achieve.

One important caveat, however, is that we have applied the above argument to the photo-heating around individual quasars only. Over longer timescales, the integrated effect of photons emitted by distant quasars with highly filtered spectra could produce a more gradual yet larger IGM temperature boost. However, we shall see it is quite difficult to reionise the IGM with *only* hard photons, so the actual temperature boost will likely be even smaller than these estimates. We address this issue in more detail in §4.

#### 4 THE FILTERING OF He II IONISING RADIATION THROUGH AN INHOMOGENEOUS IGM

Thus far we have focused on the expected temperature boost in the IGM without explicitly quantifying the *amount* of filtering which occurs through an optically thick, inhomogeneous IGM. Furthermore, we have not considered *where* in the IGM these hard photons are subsequently absorbed. In this section, we consider some simple analytical arguments for the amount of filtering expected, and the fate of hard photons. While less rigorous, these serve to motivate the detailed numerical calculations that follow later, and promote physical intuition.

Specifically, we shall address two key arguments for substantial heating during He II reionisation, which we briefly restate here. Firstly, we know from the lifting of the He II Gunn-Peterson trough at  $z \sim 2.8$  along multiple lines-of-sight that most of the He II in the Universe has been reionised by this time (*e.g.* Heap et al. 2000; Shull et al. 2004; Fechner et al. 2006). Thus, all that matters is the average heat input per photo-ionisation, which as discussed earlier is simply  $\langle E \rangle_{\text{HeII}} \simeq h_{\text{p}} \nu_{\text{HeII}} / (\alpha_{\text{s}} - 1)$  for an optically thick IGM. This has to be true from a simple energy conservation standpoint, and implies significant heating. Secondly, the spacing between quasars is much larger than the spacing between He II Lyman limit systems, which dominate the He II opacity (Abel & Haehnelt 1999; Miralda-Escudé et al. 2000). Thus, most of the IGM is exposed to filtered, hardened radiation. While such radiation is undoubtedly weakened, even if the photo-ionisation rate is low over long periods of time it may again still be possible to achieve substantial heating from a weak but persistent and hard ionising background. Thus, while we have so far demonstrated that it is difficult to achieve a large temperature boost globally in the IGM over short timescales, it still appears to be possible over longer periods of time.

While the latter scenario is certainly feasible, there are a number of uncertainties and caveats, which have not been emphasised in the literature. In particular: (i) while the average energy per ionisation in an optically thick IGM is indeed  $\langle E \rangle_{\text{HeII}} \simeq h_{\text{p}} \nu_{\text{HeII}} / (\alpha_{\text{s}} - 1)$ , dense regions preferentially absorb hard photons. The energy per photo-ionisation in the low density regions may therefore be systematically less than the average, since the average heat input in the observable IGM depends on the relative collective opacity of optically

thin and thick systems. Note that virtually all statistical measures of temperature in the H I Ly $\alpha$  forest are sensitive to the optically thin, underdense to mildly overdense regions. As an example, the low column density Ly $\alpha$  forest (where Doppler line widths are directly measurable) corresponds to regions of fairly low overdensity (Schaye 2001). (ii) There are many generations of quasars. While at any given time a patch of the IGM may be exposed only to filtered radiation, over many generations a nearby quasar will eventually be able to directly ionise that patch with only modestly filtered radiation. Reionising the IGM exclusively via soft photons does not require an unrealistic photon budget, even with a substantial population of Lyman limit systems.

#### 4.1 The fate of the hardest photons

Why should hard photons be preferentially absorbed in dense systems? We can gain some physical insight from a simple toy model. Let us consider a uniform IGM filled with a single population of absorbers of fixed mass and some overdensity  $\Delta$ . For this population, the radial size of the absorbers  $R \propto \Delta^{-1/3}$ , and hence the optical depth  $\tau \propto N_{\text{HeII}} \propto \Delta^{2/3}$ . The effective optical depth due to the absorbers has two interesting limits. When  $\Delta$  is low so that the absorbers are optically thin,  $\tau_{\text{eff}} = \sum \tau_i = N \langle \tau \rangle$ , where  $N \propto \sigma_{\text{absorber}} \propto \Delta^{-2/3}$  is the mean number of absorbers encountered along a line-of-sight,  $\langle \tau \rangle$  is the mean optical depth of a single absorber, and  $\sigma_{\text{absorber}}$  is the absorber cross-section. In this limit, the effective optical depth is independent of the overdensity  $\Delta$  of absorbers:  $\langle \tau \rangle \propto \Delta^{2/3}$ , but for increasing overdensity their cross-section falls, and thus fewer absorbers,  $N \propto \Delta^{-2/3}$ , are encountered along a line-of-sight. On the other hand, once the absorbers become optically thick, their contribution to the opacity saturates, and  $\tau_{\text{eff}} = N = X_{\text{HeII}}^{\text{absorber}} / \langle \tau \rangle \propto \Delta^{-2/3}$ , where  $X_{\text{HeII}}^{\text{absorber}} = \tau_{\text{absorber}} / \tau_{\text{IGM}}$  is the total mass fraction of He II in the absorbers. This implies that

$$\frac{\tau_{\text{absorber}}}{\tau_{\text{IGM}}} \simeq X_{\text{HeII}}^{\text{absorber}} \frac{1}{\max(1, \langle \tau \rangle)}. \quad (15)$$

Thus, on average fewer photons are absorbed in optically thick absorbers, since only the photosphere ( $\tau_{\nu} \sim 1$ ) contributes to the opacity. For hard photons the absorbers are optically thin, while for soft photons the absorbers are optically thick. Thus, a greater fraction of hard photons are absorbed by dense absorbers, rather than the IGM, compared to soft photons. Similarly, in the interstellar medium of galaxies, continuum photons can have a higher probability of being absorbed by dusty atomic/molecular clouds (which are optically thin at these frequencies), compared to Ly $\alpha$  photons, for which the clouds are optically thick (Hansen & Oh 2006).<sup>3</sup>

From the above, it is clear that the relative absorption of hard and soft photons depends on the abundance

of optically thick systems, with column densities which depend on frequency as  $N_{\text{HeII}} = 1/\sigma_{\nu} \propto \nu^3$ . In particular, the fate of hard photons depends strongly on the abundance of high column density systems, which are optically thick to photons just above the Lyman edge, but optically thin to hard photons. Unfortunately, unlike the hydrogen Ly $\alpha$  forest, it is not possible to directly observe the column density distribution  $f(N_{\text{HeII}}, z)$  of the He II forest in the UV. One is therefore forced to theoretical models of  $f(N_{\text{HeII}}, z)$  (Haardt & Madau 1996; Fardal et al. 1998). There are a number of subtle modifications which need to be made to such models while He II reionisation is in progress, and we present detailed calculations elsewhere (Oh et al. 2009, in prep.).

For now, we merely remark that  $f(N_{\text{HeII}}, z)$  can be significantly model dependent, and point out the implications of these uncertainties. The effective optical depth experienced by a photon which has frequency  $\nu_0$  at redshift  $z_0$  between redshifts  $(z_0, z_1)$  due to discrete, Poisson distributed clouds is (Paresce et al. 1980; Zuo & Phinney 1993)

$$\tau_{\text{eff}}(\nu_0, z_0, z_1) = \int_{z_0}^{z_1} dz \int_0^{\infty} dN_{\text{HI}} f(N_{\text{HI}}, z) [1 - e^{-\tau_{\nu}}], \quad (16)$$

where  $\tau_{\nu} \approx N_{\text{HI}}(\sigma_{\nu}^{\text{HI}} + \eta\sigma_{\nu}^{\text{HeII}})$ , the frequency  $\nu = \nu_0(1+z)/(1+z_0)$ , and  $\eta \equiv N_{\text{HeII}}/N_{\text{HI}}$ . Note it is generally assumed that the He I opacity is negligible (Miralda-Escude & Ostriker 1992; Haardt & Madau 1996; Fardal et al. 1998), although there may be regimes where this is not justified. While the H I column density distribution  $f(N_{\text{HI}}, z)$  is observationally determined as a function of redshift,  $\eta$  is not. Thus, above 4 Ry,  $\tau_{\text{eff}}$  depends strongly on the unknown function  $\eta(N_{\text{HI}}, z)$ . Given a model for  $\eta(N_{\text{HI}}, z)$  – which usually depends on  $\Gamma_{\text{HI}}$ ,  $\Gamma_{\text{HeII}}$  and  $n_{\text{H}}$  – and an assumed ionising source population of quasars and galaxies,  $\Gamma_{\text{HI}}$  and  $\Gamma_{\text{HeII}}$  can be self-consistently computed as a function of redshift. The coupled equations have to be solved iteratively (Haardt & Madau 1996), since the opacity depends on the ionising background and vice-versa. While  $\Gamma_{\text{HI}}$  can be compared to observations of the Ly $\alpha$  forest,  $\Gamma_{\text{HeII}}$  cannot above  $z \sim 3$ , when absorption in the He II forest saturates. This is unfortunate: the mean free path of He II ionising photons and hence  $\Gamma_{\text{HeII}}$  evolves strongly during He II reionisation, a fact which can cause considerable uncertainty in the redshift evolution of  $\eta$ .

Let us consider the qualitative behaviour of  $\eta(N_{\text{HI}}, z)$  (Haardt & Madau 1996; Fardal et al. 1998). In the optically thin limit,  $\eta = (f_{\text{HeII}} n_{\text{He}}) / (f_{\text{HI}} n_{\text{H}}) \approx (1/12)(\Gamma_{\text{HI}}/\Gamma_{\text{HeII}})$ , where  $f_i$  is the ionisation fraction and  $\Gamma_i$  is the ionising background for a given ion. In this case,  $\eta$  is a constant independent of  $N_{\text{HI}}$ . However, this is no longer true at higher column densities. At some point, He II becomes self-shielding and He III recombines, causing  $\eta$  to rise above the optically thin value. At even higher column densities, H II recombines and  $\eta \propto N_{\text{HI}}^{-1}$  plummets drastically. This modulation of  $\eta$  with  $N_{\text{HI}}$  has been modelled by radiative transfer calculations of slabs illuminated by ionising radiation on both sides (Haardt & Madau 1996; Fardal et al. 1998). The results depend on assumptions about  $\Gamma_{\text{HI}}$  and  $\Gamma_{\text{HeII}}$ , but also crucially the gas density  $n_{\text{H}}$ , which then requires an uncertain and model-dependent correspondence to be made between  $n_{\text{H}}$  and  $N_{\text{HI}}$ . For instance, in the widely used mod-

<sup>3</sup> Another instance of this saturation of the opacity of optically thick absorbers comes from the well known fact that the mean transmission of Ly $\alpha$  photons is always larger in a clumpy IGM compared to a uniform IGM, so that the transmission is always dominated by underdense voids (e.g. Fan et al. 2002). All this stems from the triangle inequality,  $\langle \exp[-\tau] \rangle \leq \exp[-\langle \tau \rangle]$ .

els of Haardt & Madau (1996), which assume separate fixed densities for Ly $\alpha$  systems above and below the self-shielding limit  $N_{\text{HI}} = 1.6 \times 10^{17} \text{ cm}^{-2}$ , this turnover takes place at  $N_{\text{HI}}^* = 1.2 \times 10^{18} \text{ cm}^{-2}$ . On the other hand, McQuinn et al. (2008), following the *ansatz* of Schaye (2001), assume that  $n_{\text{H}} \propto N_{\text{HI}}^{2/3}$ , and instead find that the turn-over takes place at  $N_{\text{HI}}^* = 10^{15} - 10^{16} \text{ cm}^{-2}$ , depending on the assumed value of  $\Gamma_{\text{HeII}}$ .

This model-dependence has little impact on self-consistent calculations of  $\Gamma_{\text{HeII}}$  (at least once He II reionisation is complete). This is because He II ionising photons are strongly weighted toward the Lyman edge, and the turn-over in  $\eta$  only takes place in systems which are already optically thick to photons at  $\sim 4$  Ry. For such photons, it does not really matter whether the optical depth of a system is  $\tau \sim 2$  or  $\tau \sim 4$ ; the high absorption probability changes only slightly. For this reason, previous studies correctly did not regard this model-dependence as a liability. On the other hand, for higher energy photons—for which such systems are still optically thin—the exact column density *is* important, since  $\tau \propto N_{\text{HeII}}$  in this regime. This in turn translates into considerable uncertainty about the frequency dependence of the opacity, and hence the spectral shape of He II ionising background and the photo-heating of the IGM.

For instance, let us consider the mean excess energy per He II photo-ionisation

$$\begin{aligned} \langle E \rangle_{\text{HeII}} &= \frac{\epsilon_{\text{HeII}}}{\Gamma_{\text{HeII}}} = \frac{\int_{\nu_{\text{HeII}}}^{\infty} d\nu h_{\text{p}}(\nu - \nu_{\text{HeII}}) \epsilon_{\nu} \lambda_{\nu} \sigma_{\nu}}{\int_{\nu_{\text{HeII}}}^{\infty} d\nu \epsilon_{\nu} \lambda_{\nu} \sigma_{\nu}} \\ &\simeq \frac{h_{\text{p}} \nu_{\text{HeII}}}{(\alpha_{\text{s}} - \xi + 2)}. \end{aligned} \quad (17)$$

Here  $\epsilon_{\nu} \propto \nu^{-\alpha_{\text{s}}-1}$  is the He II ionising emissivity [photons  $\text{cm}^{-3} \text{ s}^{-1} \text{ Hz}^{-1}$ ],  $\lambda_{\nu} \propto \nu^{\xi}$  is the mean free path for He II ionising photons and  $\sigma_{\nu} = \sigma_0 (\nu_0 / \nu_{\text{HeII}})^{-3}$ , where  $\sigma_0 = 1.5 \times 10^{-18} \text{ cm}^2$  is the photo-ionisation cross-section at the He II ionisation threshold. For a uniform optically thick IGM,  $\lambda_{\nu} \propto \nu^3$  and  $\langle E \rangle_{\text{HeII}} \simeq h_{\text{p}} \nu_{\text{HeII}} / (\alpha_{\text{s}} - 1)$ , while for the optically thin case,  $\lambda_{\nu}$  is constant and comparable to the size of the system under consideration, yielding  $\langle E \rangle_{\text{HeII}} \simeq h_{\text{p}} \nu_{\text{HeII}} / (\alpha_{\text{s}} + 2)$ . Of course, the full inhomogeneous density structure of the IGM must be taken into account, using eq. (16). If we ignore the effect of He III continuum recombination radiation (which can significantly soften the spectrum), the widely used model of Haardt & Madau (1996) yields  $\lambda \propto \nu^{1.5}$ , and hence  $\langle E \rangle_{\text{HeII}} \simeq h_{\text{p}} \nu_{\text{HeII}} / (\alpha_{\text{s}} + 0.5)$  (F. Haardt, private communication). This level of heating is intermediate between the optically thick and optically thin case. The result is easy to understand: the turnover in  $\eta$  occurs at high values of  $N_{\text{HI}}$ , and the assumption of constant  $\eta$  is a reasonable first approximation. Doing so, and assuming that  $f(N_{\text{HI}}, z) \propto N_{\text{HI}}^{-\beta}$ , we obtain:

$$\tau_{\text{eff}} = [\Gamma(\beta - 1), 1] \left( \frac{\lambda}{\lambda_{\text{LL}}} \right) \left( \frac{\nu}{\nu_{\text{HeII}}} \right)^{-3(\beta-1)}, \quad (18)$$

where  $\lambda$  is the comoving distance travelled by the photon,  $\lambda_{\text{LL}}$  is the mean free path at the He II Lyman limit and the term in the brackets apply when  $N_{\text{min}} = [0, \sigma_0^{-1}]$ . Note here that  $\Gamma$  (with no subscript) represents the gamma function. For  $\beta = 1.5$ , as assumed by Haardt & Madau (1996) in the relevant regime  $N_{\text{min}} = \sigma_0^{-1}$ , we therefore

obtain  $\tau_{\text{eff}} \propto \nu^{-1.5}$ , or  $\lambda_{\nu} \propto \nu^{1.5}$ . On the other hand, the assumption of constant  $\eta$  is not appropriate for models where  $\eta$  turns over at much lower column densities  $N_{\text{HI}}$ . For instance, in the modified version of the model presented by McQuinn et al. 2008 in which  $n_{\text{H}} \propto N_{\text{HI}}^{2/3}$ , we obtain  $\langle E \rangle \simeq h_{\text{p}} \nu_{\text{HeII}} / (\alpha_{\text{s}} - 0.5)$ , assuming  $\Gamma_{\text{HeII}} = 10^{-14} \text{ s}^{-1}$ . Accounting for the thermalisation between all species, this corresponds to a temperature jump of  $\Delta T \approx 15 \text{ 000 K}$ : less than the optically thick number of  $\Delta T \approx 30 \text{ 000 K}$ , but also significantly greater than the  $\Delta T \approx 7000 \text{ K}$  associated with the Haardt & Madau (1996) model for  $\eta$ . These uncertainties ultimately have to be observationally resolved.

To summarise: *if* high  $N_{\text{HeII}}$  column density systems are abundant, then most high energy photons will be deposited there. However, the abundance of such systems—particularly during the course of He II reionisation—is far from clear, leading to considerable uncertainty in heating rates. We will consider the effect of dense clumps on photo-heating further in §6 using our radiative transfer simulations.

## 4.2 Reionising He II with the softer photons

The second key argument for the importance of filtered radiation is the fact that the spacing between quasars is much less than the spacing between He II Lyman limit systems (Abel & Haehnelt 1999). Let us consider an updated version of this argument. At  $z \sim 3$ , quasars with  $L_{\text{B}} \sim L_* \simeq 10^{12} L_{\odot}$  dominate the photon budget (Furlanetto & Oh 2008b). These have a space density of  $n_{\text{q}} \sim 10^{-6} \text{ Mpc}^{-3}$ , or a mean separation of  $n^{-1/3} \sim 100 \text{ Mpc}$ . Let us now reasonably suppose that these quasars can only directly ionise the IGM out to distances where they will on average encounter a self-shielded Lyman limit system. Assuming the typical size of an absorber with overdensity  $\Delta$  is the local Jeans length, then in ionisation equilibrium its He II column density is approximately given by (Schaye 2001)

$$N_{\text{HeII}} \simeq 1.6 \times 10^{15} \text{ cm}^{-2} \frac{\Delta^{3/2}}{\Gamma_{-14}} \left( \frac{T}{10^4 \text{ K}} \right)^{-0.2} \left( \frac{1+z}{4} \right)^{9/2}, \quad (19)$$

where  $\Gamma_{-14} = \Gamma_{\text{HeII}} / 10^{-14} \text{ s}^{-1}$ . The clump will then become self-shielded once  $N_{\text{HeII}} > 1/\sigma_0 = 6.7 \times 10^{17} \text{ cm}^{-2}$ . This corresponds to a characteristic overdensity (Furlanetto & Oh 2008b)

$$\Delta_i \simeq 56 \left( \frac{T}{10^4 \text{ K}} \right)^{2/15} \left( \frac{1+z}{4} \right)^{-3} \Gamma_{-14}^{2/3}. \quad (20)$$

Miralda-Escudé et al. (2000) provide a prescription for estimating the separation between clumps of overdensity  $\Delta > \Delta_i$  calibrated to numerical simulations at  $z = 2-4$ . In their model, the separation between clumps of density  $\Delta_i$  is given by

$$\begin{aligned} \lambda_i &= \lambda_0 (1+z) [1 - F_{\text{V}}(\Delta_i)]^{-2/3}, \\ &\simeq 82 \text{ Mpc} \left( \frac{\Delta_i}{50} \right) \left( \frac{1+z}{4} \right), \end{aligned} \quad (21)$$

where  $F_{\text{V}}(\Delta_i)$  is the fraction of volume with  $\Delta < \Delta_i$ , and  $\lambda_0 H(z) = 60 \text{ km s}^{-1}$  is a good fit to their simulations. The second equality uses the fact that the Miralda-Escudé et al. (2000) density distribution rapidly approaches an isothermal profile at high densities,  $\rho \propto r^{-2}$ , and provides an excellent approximation to their expression at  $z = 3$  (see the appendix

of Furlanetto & Oh 2005). Setting  $R = \lambda(\Delta_i)$  and using eqs. (12), (20) and (21), we thus find that a photon at the He II Lyman edge can travel a comoving distance

$$R_{\text{lim}} \simeq 30 \text{ Mpc} \left( \frac{L}{10^{12} L_{\odot}} \right)^{2/7} \left( \frac{1+z}{4} \right)^{-2/7}, \quad (22)$$

before it is absorbed by a Lyman limit system. We have ignored the weak dependence ( $R_{\text{lim}} \propto T^{2/35}$ ) on temperature in this expression. Since  $R_{\text{lim}} \sim 30 \text{ Mpc} < n^{-1/3} \sim 100 \text{ Mpc}$ , it would appear that most of the IGM is inevitably exposed to filtered, hardened radiation (Abel & Haehnelt 1999). While such filtered radiation is undoubtedly weak and results in a low photo-ionisation rate (see §3), over long periods of time, it may still seem possible to achieve substantial heating.

However, there are some caveats to this argument. The mean separation between  $L_*$  quasars is not the correct metric in this instance. The region over which a quasar ionises He II is generally substantially less than  $n^{-1/3}$ . Instead, He II must become reionised over many generations of quasar formation, since the lifetime of quasars,  $t_s \sim 10^6 - 10^8 \text{ yrs}$  (Martini 2004), is much less than the Hubble time. Again for  $\alpha_s = 1.5$ , a quasar can ionise a region of radius

$$R_i \simeq \frac{32 \text{ Mpc } f_{\text{abs}}^{1/3}}{(\Delta f_{\text{HeII}})^{1/3}} \left( \frac{L_B}{10^{12} L_{\odot}} \right)^{1/3} \left( \frac{t_s}{10^8 \text{ yrs}} \right)^{1/3}, \quad (23)$$

where  $f_{\text{abs}}$  is the fraction of photons absorbed within the He III region. We have again taken the *upper limit* for the quasar lifetime to be conservative with regard to the maximum temperature boost. Since  $R_i \lesssim R_{\text{lim}} < n^{-1/3}$ , most of the photons that ionised the IGM need not have undergone significant filtering, at least until  $f_{\text{HeII}} < 0.1$ . Note that this requirement becomes even stricter if the quasars have shorter lifetimes than  $10^8 \text{ yrs}$ .<sup>4</sup> Instead, most photons photo-ionise and heat the region directly around their source quasar. Significant photo-heating by strongly filtered radiation is thus more likely to occur towards the end of He II reionisation, once most of the He II is reionised. Even then, as discussed previously, much of this heating could potentially occur in the Lyman limit systems themselves. Again, it appears difficult to reionise the entire IGM *exclusively* with hard photons and hence achieve a large, global temperature boost.

One worry with this argument might be that the photon budget for successive generations of quasars to reionise the IGM is prohibitive. If every quasar only ionises a fixed, local region of the IGM, as implied above, then are there enough photons available to complete reionisation? To be conservative we will assume  $R_{\text{lim}} \rightarrow R_i$ . Then, if the filling fraction of ionised He III regions is  $Q_i$ , on average a quasar will only be able to freshly reionise a new volume  $V_i(1 - Q_i)$  around it.<sup>5</sup> The rest of the photons are consumed by Lyman

<sup>4</sup> Note the very similar scaling with luminosity of  $R_{\text{lim}} \propto L^{2/7}$  and  $R_i \propto L^{1/3}$ ; hereafter we shall ignore this difference.

<sup>5</sup> Note that this assumes quasars are Poisson distributed. Clustering can clearly increase this penalty somewhat, since it increases the probability that a quasar is born in a previously ionised region. However, since the correlation length,  $r_0 = 15.2 \pm 2.7 h^{-1} \text{ Mpc}$ , for the relatively luminous quasars observed with

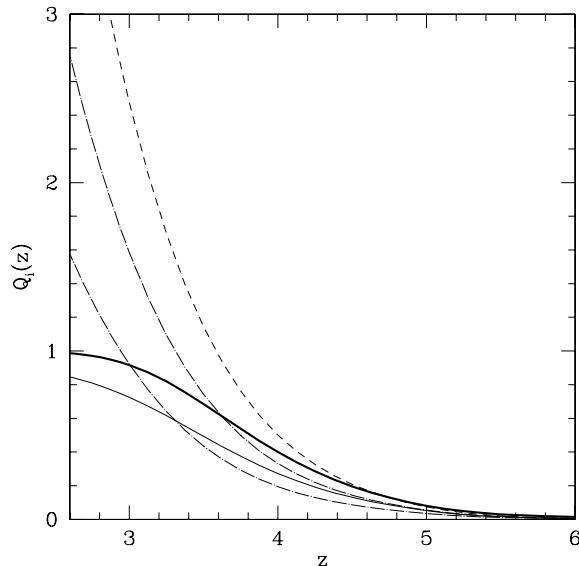


**Figure 2.** Reionisation histories for He II assuming an ionising emissivity derived from the Hopkins et al. (2007) quasar luminosity function. The volume filling factor of ionised He III regions,  $Q_i(z)$ , is shown in the case of no photon sinks (dashed curve), recombinations as in eq. (25) with  $\bar{C} = 1, 3$  (dot-dashed curves), Lyman limit systems as in eq. (24) (thick solid curve) and both photon sink terms with  $\bar{C} = 1$  (thin solid curve). The fact that Lyman limit systems only allow quasars to ionise a fixed volume, regardless of their previous ionisation history (as represented by eq. 25), does not incur a significant photon cost, and He II reionisation can still continue to completion.

limit systems in the existing ionised regions. By taking this photon sink due to He II Lyman limit systems into account (and ignoring all other sinks), the filling factor evolves as

$$\dot{Q}_i = \dot{n}_i(1 - Q_i), \quad (24)$$

where  $\dot{n}_i$  is the rate at which He II ionising photons are produced per helium atom. Note that this differs from the customary relation

$$\dot{Q}_i = \dot{n}_i - RQ_i, \quad (25)$$

(Madau et al. 1999; Miralda-Escudé et al. 2000), where  $R(t)$  is the average recombination rate per atom in ionised regions which also includes the effective clumping factor,  $\bar{C}$ , of ionised gas. Instead, eq. (24) ignores the effect of recombinations in the IGM and only considers the Lyman limit systems as a photon sink. It mimics the effect that  $\bar{C}$  must increase rapidly as  $Q_i \rightarrow 1$  when dense pockets of gas must begin to be ionised (Furlanetto & Oh 2005); quasar He III regions are sufficiently large that this could potentially happen at all stages of the reionisation process. Note also that since the recombination time in underdense regions of the IGM is long, fossil He III cavities which were ionised by extinct quasars far outnumber active He III regions during reionisation (Furlanetto et al. 2008, see also §5). The ionising emissivity required to *keep* the IGM ionised should thus be sig-

the Sloan Digital Sky Survey at  $z > 2.9$  (Shen et al. 2007) is comparable to  $R_i$ , we expect this to be an order unity effect.

nificantly less than that required to initially reionise it, and can be maintained by the active generation of quasars.

In Fig. 2 we show the evolution of  $Q_i(z)$  according to these two equations, where we have computed the ionising emissivity using the Hopkins et al. (2007) luminosity function. The result for no photon sinks is shown by the dashed curve, the dot-dashed curves include recombinations as in eq. (25) with  $\bar{C} = 1, 3$ , the thick solid curve includes the sink due to Lyman limit systems as in eq. (24) (but not recombinations), and the result including both photon sink terms (recombinations and Lyman limit systems) with  $\bar{C} = 1$  is indicated by the thin solid curve. Note that since  $Q_i(z)$  is simply the number of ionising photons produced minus the photon sink terms, it can exceed unity once reionisation is complete, at least in the case of eq. (25).

The most important point to take away is that allowing quasars to only ionise a fixed volume, regardless of the previous ionisation history of their surroundings, does not incur a large cost in the photon budget and He II reionisation can still continue to completion. Most of the IGM can therefore be reionised by a direct source of soft photons; there are few isolated patches which have only been exposed to hard photons (and hence which are heated significantly). It is also worth noting that photo-ionisation timescales are then likely to be short. Unlike hydrogen reionisation, the size of He III regions are already controlled by He II Lyman limit systems before overlap, since  $R_i \sim R_{\text{lim}}$ . Hence, the mean free path and thus the ionising radiation field can only increase mildly – at best by a factor of 2 or 3 – during percolation. The strength of the radiation field after overlap is constrained by transmission along all lines-of-sight in the He II Gunn Peterson trough. The results of Zheng et al. (2004) suggest a fit to the He II effective optical depth of  $\tau_{\text{eff}} \simeq 1.[(1+z)/3.8]^{3.5}$  for  $z < 2.8$ , or  $\Gamma_{\text{HeII}} \simeq 10^{-14} \text{ s}^{-1}$ . This ionising background implies ionisation timescales of  $\Gamma_{\text{HeII}}^{-1} \sim 3 \times 10^6 \text{ yr} \ll t_{\text{H}}$ . This directly contradicts the possibility that most of the IGM is pervaded by weak, filtered radiation; instead, most or all of the IGM must lie within the proximity zone of bright source(s) which gives rise to a strong ionising radiation field. Such sources at a slightly earlier epoch would cause rapid He II ionisation.

## 5 PHOTO-HEATING IN FOSSIL He III REGIONS

Thus far we have considered photo-heating in regions of the IGM where He II is reionised only once. However, Furlanetto et al. (2008) have recently pointed out that fossil He III regions will be common during the epoch of He II reionisation; less than 50 percent of the He III created by dead quasars will have enough time to recombine before another quasar appears. The time lag between successive ionisations of a patch of the IGM is  $t_{\text{lag}} \sim 7 \times 10^7 \text{ yrs}$  at  $z = 3$  (Furlanetto et al. 2008), based on the expected number density of  $L \geq 10^{11.5} L_{\odot}$  quasars from Hopkins et al. (2007). Could a second round of He II reionisation in a partially recombined fossil He III region then boost the IGM temperature even further, leading to temperatures in excess of those otherwise expected from our previous arguments?

The case-B He III recombination timescale,  $t_{\text{rec}} = (\alpha_{\text{HeIII}} n_e)^{-1}$ , can be written as

$$t_{\text{rec}} \simeq \frac{1.4 \times 10^9 \text{ yrs}}{\Delta} \left( \frac{T}{10^4 \text{ K}} \right)^{0.7} \left( \frac{1+z}{4} \right)^{-3}, \quad (26)$$

whereas the time to replenish a given He II fraction,  $f_{\text{HeII}}^{\text{rep}}$ , is  $t_{\text{rep}} \approx f_{\text{HeII}}^{\text{rep}} t_{\text{rec}}$ . The He II fraction replenished in  $t_{\text{lag}} \sim 7 \times 10^7 \text{ yrs}$  is thus  $f_{\text{HeII}}^{\text{rep}} \sim 0.05$  for  $\Delta = 1$  and  $T = 10^4 \text{ K}$ . Note further from eq. (7) that the temperature increase due to He II photo-heating is proportional to  $f_{\text{HeII}}$ . Thus, since the recombination time in voids filled with He III is so long compared to  $t_{\text{lag}}$ , they will only experience a small fraction of the heating achieved during the first round of He II reionisation. In contrast, clumps with  $\Delta > 20$  have sufficient time to recombine nearly completely before undergoing a second phase of He II reionisation, potentially allowing the He II to be fully reheated for a second time.

However, we must also consider the cooling timescale to establish whether any *additional* temperature increase is actually achieved following a second He II reionisation. If  $t_{\text{cool}} < t_{\text{rec}}$ , even if a clump in the fossil region has had sufficient time to fully recombine such that  $t_{\text{rec}} < t_{\text{lag}}$ , the IGM will have cooled more quickly and any subsequent photo-heating by a quasar can, at most, only restore the previous temperature in the He III region.<sup>6</sup> Fig. 3 displays the recombination and cooling timescales as a function of temperature for gas of primordial composition at  $z = 3$  in photo-ionisation equilibrium with a UV background specified by

$$J_{\nu} = J_{-21} \left( \frac{\nu}{\nu_{\text{HI}}} \right)^{-\alpha_{\text{b}}} \times \begin{cases} 1 & (\nu_{\text{HI}} \leq \nu < \nu_{\text{HeII}}), \\ 0 & (\nu_{\text{HeII}} \leq \nu), \end{cases} \quad (27)$$

where  $J_{-21} = 0.5$  and  $\alpha_{\text{b}} = 3$ . The amplitude is consistent with measurements of the H I photo-ionisation rate at  $z = 2-4$  based on the observed Ly $\alpha$  forest opacity (Bolton et al. 2005). The solid curves show the radiative cooling timescale

$$t_{\text{rad}} = T \left( \frac{dT}{dt} \right)^{-1} \simeq \frac{3\rho k_{\text{B}} T}{2\mu m_{\text{H}} (\Lambda - \mathcal{H})}, \quad (28)$$

at three different IGM densities. The cooling rate is computed using the rates listed in Bolton & Haehnelt (2007a), with the exception of the case-B recombination cooling rates which use the functions given by Hui & Gnedin (1997). The dashed curves display the corresponding case-B He III recombination timescale. The minimum in the radiative cooling timescale at  $T \sim 10^{4.9} \text{ K}$  results from He II excitation cooling, while the high temperature tail is due to the inverse Compton scattering of free electrons off cosmic microwave background photons. The horizontal dotted line shows the adiabatic cooling timescale for the low density gas which is still expanding with the Hubble flow ( $\Delta \lesssim 10$ ). For temperatures  $T > 10^4 \text{ K}$  at  $\Delta = 1$ , the recombination time exceeds the adiabatic cooling timescale. Hence, the IGM temperature in the voids following a second reheating will in general be smaller than the temperature immediately following the initial reionisation, irrespective of the time lag between successive ionisations.

At higher densities, adiabatic expansion will no longer dominate the cooling timescale for clumps which have already separated from the Hubble flow. In this instance, radiative cooling becomes dominant, and the cooling timescale

<sup>6</sup> The exception to this is if the second quasar has an intrinsic spectrum which is substantially harder than the quasar that originally created the fossil He III region.

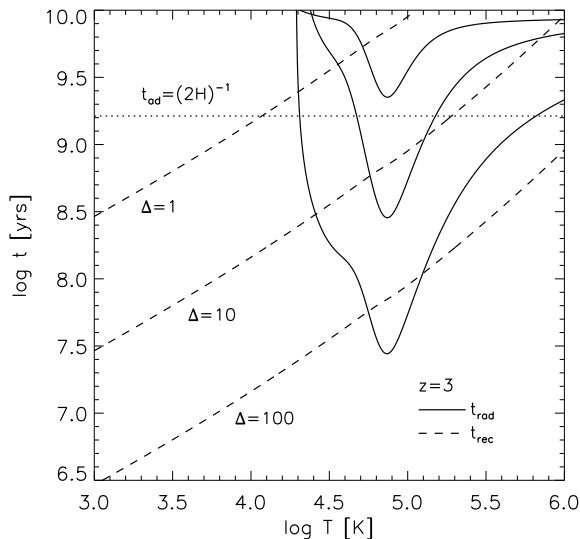


**Figure 3.** Recombination and cooling timescales as a function of temperature for gas of primordial composition at  $z = 3$  in photo-ionisation equilibrium with the UV background given by eq. (27). The solid curves show the radiative cooling timescale at three different densities, from top to bottom  $\Delta = (1, 10, 100)$ , while the dashed curves display the corresponding case-B He III recombination timescale as labelled on the figure. The horizontal dotted line shows the adiabatic cooling timescale for low density gas still expanding with the Hubble flow ( $\Delta \lesssim 10$ ).

falls below the recombination timescale for  $T > 10^{4.7}$  K. Furthermore, the cooling timescale becomes comparable to the time lag between successive ionisations at  $z = 3$  for  $\Delta = 100$ . If  $t_{\text{cool}} < t_{\text{lag}}$ , even high density clumps in the fossil He III region which can recombine efficiently are unlikely to receive a substantial *additional* temperature boost following a second reheating. Note further that the radiative cooling timescale in overdense regions of the IGM is likely to be even shorter than we have assumed here. Although the assumption of primordial composition is a reasonable approximation for voids in the IGM, metals are ubiquitous in higher density regions (*e.g.* Pettini 2004) and substantially increase the radiative cooling rate, depending on their abundance (Maio et al. 2007; Smith et al. 2008; Wiersma et al. 2008). This would make any net temperature increase even more difficult to achieve.

Finally, at higher redshifts the time lag between successive ionisations for a given patch of the IGM increases as the quasar number density drops; Furlanetto et al. (2008) estimate  $t_{\text{lag}} \sim (1.4, 7.2) \times 10^8$  yrs at  $z = (4, 5)$ . On the other hand, the recombination and He II collisional excitation cooling timescales at fixed density decrease as  $(1+z)^3$ . Hence, at higher redshifts the fossil region is even more likely to have sufficient time to recombine and cool before another quasar can reheat the IGM. We conclude that partially or fully recombined fossil He III regions which are reheated a second time are therefore unlikely to exhibit temperatures in excess of those expected following the initial phase of He II reionisation. Note however, heating in these regions is

still likely to contribute significantly to the *complexity* of the relationship between temperature and density in the IGM during He II reionisation (see §7).

## 6 RADIATIVE TRANSFER THROUGH AN INHOMOGENEOUS IGM

### 6.1 Numerical code

In the previous sections we have employed analytical arguments to model the photo-heating of the IGM during He II reionisation. However, detailed radiative transfer simulations (ideally, with a full three-dimensional, multi-frequency approach) are required to fully address this problem. Unfortunately, such simulations are computationally challenging, requiring very high spatial resolution within large simulation volumes in order to accurately track the topology of He II reionisation, as well as high frequency resolution to correctly follow the thermal state of the IGM. Existing calculations are thus either one dimensional (Haardt & Madau 1996; Abel & Haehnelt 1999; Bolton et al. 2004; Bolton & Haehnelt 2007a), neglect the modelling of multiple sources (Maselli & Ferrara 2005; Tittley & Meiksin 2007), or resort to approximation schemes which do not recover the reprocessing of the ionising radiation field precisely (Sokasian et al. 2002; Paschos et al. 2007). The latter is crucial for correctly modelling the IGM thermal evolution. High spatial resolution is also needed to resolve the overdense regions in the IGM which play an important role in filtering the ionising radiation. Furthermore, large, computationally expensive simulations allow only a limited parameter space to be explored.

We therefore explore the results discussed previously using an updated version of the one-dimensional, multi-frequency photon conserving algorithm described and tested in Bolton et al. (2004) and Bolton & Haehnelt (2007a). This approach is based on the monochromatic photon-conserving algorithm originally developed by Abel et al. (1999). Note that our simulations do not model He II reionisation using large volumes (*e.g.* Paschos et al. 2007; McQuinn et al. 2008) and will therefore not correctly capture any three dimensional effects such as long range photo-heating by multiple quasars. Instead, our models employ very high spatial and mass resolution and thus resolve the dense regions in the IGM which are important for filtering the ionising radiation. This high resolution is computationally prohibitive in larger, three dimensional simulations.

The frequency integration in the updated code is now performed over the range  $13.6 \text{ eV} < h_p \nu < 1 \text{ keV}$ , allowing the simulations to follow the radiative transfer of soft X-ray and UV photons. Photons with energies in excess of 1 keV are relatively rare and do not contribute significantly to photo-heating in the IGM over a typical quasar lifetime. Secondary ionisations are included following the prescription of Ricotti et al. (2002), and the photo-ionisation cross-sections from Verner et al. (1996) are now used instead of the fits from Osterbrock (1989). Our one-dimensional radiative transfer code does not follow the diffuse emission from recombination radiation, and so an option to include the on-the-spot approximation using the case-B recombination and cooling rates of Hui & Gnedin (1997) has also been

added. In this work we shall always use the case-B values, although case-A would be the more appropriate choice in underdense, highly ionised regions of the IGM. However, in this work we only consider the reionisation of an IGM with an initial He II fraction  $f_{\text{HeII}} = 1$ , and so case-B is the more appropriate choice.

## 6.2 Initial conditions

In order to simulate the propagation of ionising radiation through the inhomogeneous IGM we use density distributions drawn from a high resolution hydrodynamical simulation run using the parallel Tree-SPH code GADGET-2 (Springel 2005). The simulation volume is a periodic cube 27.8 Mpc in length containing  $2 \times 400^3$  gas and dark matter particles. Each gas particle has a mass of  $2.24 \times 10^6 M_{\odot}$ . This mass resolution adequately resolves the Ly $\alpha$  forest at  $z = 3$  (Bolton et al. 2008). A friends-of-friends halo finding algorithm was used to identify the ten most massive haloes in the simulation volume at  $z = 3$ . The haloes span a mass range of  $6.67 \times 10^{11} M_{\odot} \leq M_{\text{halo}} \leq 2.42 \times 10^{12} M_{\odot}$  and lie above the minimum mass expected for quasars with  $L_{\text{B}} > 10^{11} L_{\odot}$  at  $z = 2-3$  (Lidz et al. 2006; Furlanetto & Oh 2008a). Density distributions were then extracted around these haloes and spliced with other lines-of-sight drawn randomly from the simulation volume at the same redshift following the procedure described in Bolton & Haehnelt (2007a). This resulted in 30 different line-of-sight IGM density distributions, all of which start at the location of one of the most massive haloes in the simulation volume. Each complete line-of-sight is 97.2 Mpc in length and is divided into 1024 equally spaced pixels in the radiative transfer calculation, giving a cell size of 94.9 kpc. At mean density at  $z = 3$  for  $f_{\text{HeII}} = 1$ , this corresponds to an He II optical depth per cell of 0.1 at the He II ionisation edge.

These density distributions are used to run a total of 270 separate line-of-sight radiative transfer simulations, divided into nine groups of 30. In all these simulations, we shall assume the H I and He I in the IGM is initially in photo-ionisation equilibrium with the UVB given by eq. (27). The first group of simulations is our fiducial quasar model with  $L_{\text{B}} = 10^{12} L_{\odot}$ ,  $\alpha_{\text{s}} = 1.5$  and  $t_{\text{s}} = 10^8$  yrs. Five further groups are run by varying one of the quasar parameters in the model: specifically  $\alpha_{\text{s}} = 0.5$ ,  $\alpha_{\text{s}} = 2.5$ ,  $L_{\text{B}} = 10^{11} L_{\odot}$ ,  $L_{\text{B}} = 10^{13} L_{\odot}$  and  $t_{\text{s}} = 10^7$  yrs. In all of these models we assume an isothermal IGM with  $T = 10^4$  K prior to He II reionisation, consistent with the measurements of Schaye et al. (2000). The final three groups again use the fiducial quasar model, plus the two models with  $\alpha_{\text{s}} = 0.5$  and 2.5. However, instead of adopting an isothermal IGM with  $T = 10^4$  K prior to the quasar turning on, a power-law temperature-density relation is adopted (*e.g.* Hui & Gnedin 1997; Valageas et al. 2002). Specifically, we set  $T = T_0 \Delta^{\gamma-1}$  for  $\Delta \leq 10$ , and  $T = T_0 10^{\gamma-1}$  for  $\Delta > 10$ , with  $T_0 = 10^4$  K and  $\gamma = 1.3$ , again consistent with the Schaye et al. (2000) data. This initial temperature distribution resembles the results from optically thin hydrodynamical simulations of the IGM (Bolton et al. 2008).

## 6.3 Six example lines-of-sight

The results for six of the simulated lines-of-sight are shown in detail in Figs. 4 and 5. The temperature of the IGM is displayed in the upper left panels, with the corresponding H I and He II fractions in the upper centre panels. The IGM density distributions along the lines-of-sight are displayed in the upper right panels. The lower panels display, from left to right, the integrated He II optical depth along the lines-of-sight for photons with energies 54.4 eV and 200 eV, the He II photo-ionisation rates and the average excess energy per He II photo-ionisation. The thin curves in the latter two panels correspond to the relevant quantities computed in the optically thin limit, while the filled circles correspond to the distance from the quasar where the He II optical depth at the He II ionisation threshold first exceeds unity. The dotted horizontal line in the lower central panel indicates the inverse of the adopted quasar lifetime,  $t_{\text{s}}$ . A selection of numerical results from the six lines-of-sight are summarised in Table 1.

In each panel of Fig. 4 the solid, dashed and dash-dotted curves correspond to the fiducial, soft and hard quasar models, respectively. The temperature for all three models increases somewhat within  $\sim 5$  Mpc of the quasar. The large gas overdensities encountered approaching the centre of the haloes (typically  $\Delta > 100$ ) strongly filter the ionising radiation, exposing the nearby IGM to very hard, intense ionising radiation for a short period of time. The analytical estimates presented in Fig. 1 are consistent with such temperature boosts occurring close to a quasar. However, once these regions have been fully ionised, this filtering disappears, so it is not important for the distant IGM.

Outside of this region, the IGM temperatures for the fiducial and soft quasar models are fairly modest, with maximum temperatures of  $T = 18\,700$  K and  $14\,500$  K occurring at  $R = 24$  Mpc and  $38$  Mpc, respectively. The temperature in the soft model corresponds to the dense clump located around  $38$  Mpc from the quasar. This is consistent with many of the hardest photons being deposited in He II Lyman limit systems, as argued in detail in §4. In the hard quasar model a dramatic boost in the IGM temperature is apparent. The maximum temperature is  $T = 34\,100$  K at  $R = 38$  Mpc, again corresponding to the overdense structure with  $\Delta \sim 50$  shown in the upper right panel. The void which appears immediately down-stream from this clump is irradiated by hard, filtered yet intense ionising radiation which photo-heats the gas to a temperature substantially higher than the mildly overdense regions closer to the quasar. Increased temperatures in the underdense regions in the IGM may be required to reconcile the observed flux distribution of the Ly $\alpha$  forest with simulations (Becker et al. 2007; Bolton et al. 2008). Note also that the presence of a second highly overdense clump at  $R \sim 47$  Mpc, which has yet to be fully ionised by the quasar, further attenuates and hardens the radiation. However, photo-heating by this very hard but weak radiation is now less effective beyond this clump, where  $\Gamma_{\text{HeII}} < t_{\text{s}}^{-1}$ .

In general the temperatures within the ionised zone all increase with distance from the quasar; regions further from the quasar are more likely to be ionised by hard photons with long mean free paths (Abel & Haehnelt 1999). The temperature then falls again beyond the He III ionisation front, where the ionisation rate declines. The average tem-

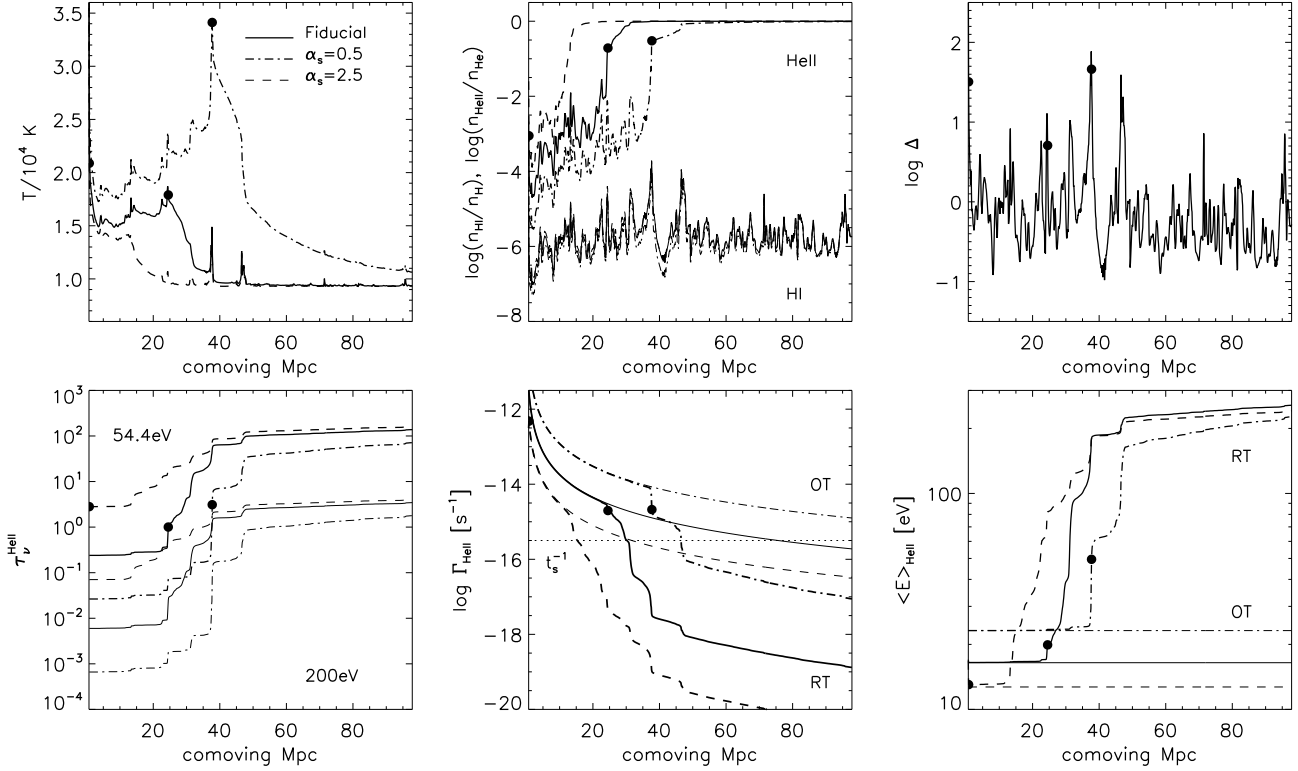


**Figure 4.** Transfer of ionising radiation emitted by a quasar with  $L_B = 10^{12} L_\odot$  through a density distribution drawn from a high resolution hydrodynamical simulation of the IGM at  $z = 3$ . The quasar is situated in a halo on the left of each panel and has an age of  $t_s = 10^8$  yrs at  $z = 3$ . The gas along the line-of-sight is initially in photo-ionisation equilibrium with a spatially uniform UV background with  $J_{-21} = 0.5$  and  $\alpha_b = 3$  between the H I and He II ionisation thresholds. Above the He II ionisation threshold the background is switched off. Three different EUV spectral indices are adopted, the fiducial model with  $\alpha_s = 1.5$  (solid curves),  $\alpha_s = 0.5$  (dash-dotted curves) and  $\alpha_s = 2.5$  (dashed curves). *Upper left:* The temperature structure at  $z = 3$  along the line-of-sight from the quasar. *Upper centre:* The H I (thin curves) and He II (thick curves) fractions along the line-of-sight. *Upper right:* The IGM density distribution. *Lower left:* The He II optical depth,  $\tau_\nu^{\text{HeII}}$ , evaluated at the He II ionisation threshold (54.4 eV) and 200 eV. *Lower centre:* The He II photo-ionisation rate. The thin curves are the rates computed in the optically thin limit, and the dotted line corresponds to the inverse of the quasar lifetime,  $t_s^{-1}$ . *Lower right:* The average excess energy per He II photo-ionisation,  $\langle E \rangle_{\text{HeII}} = \epsilon_{\text{HeII}} / \Gamma_{\text{HeII}}$ . In all panels the filled circles correspond to the comoving distance from the quasar where  $\tau_{54.4 \text{ eV}}^{\text{HeII}}$  first exceeds unity.

**Table 1.** Summary of the data presented for the six example lines-of-sight in Figs. 4 and 5. In all models the initial IGM temperature-density relation is assumed to be isothermal with  $T = 10^4$  K and the temperature boost,  $\Delta T$ , is computed accordingly. The fiducial model corresponds to a quasar with  $L_B = 10^{12} L_\odot$ ,  $t_s = 10^8$  yrs and  $\alpha_s = 1.5$ . From left to right, the columns list the model name, the mean temperature boost for all gas with  $f_{\text{HeII}} < 0.1$ , the corresponding mean excess energy per photo-ionisation computed using eq. (7), the distance from the quasar where  $\tau_{54.4 \text{ eV}}^{\text{HeII}} \sim 1$  and the corresponding normalised density, temperature boost, photo-ionisation rate and mean excess energy per photo-ionisation as a fraction of the optically thin values. The estimates for the average temperature boosts include the biased regions within  $\sim 5$  Mpc of the quasar.

Model	$\langle \Delta T \rangle$ [K] ( $f_{\text{HeII}} < 0.1$ )	$\langle E \rangle_{\text{HeII}}$ [eV] ( $f_{\text{HeII}} < 0.1$ )	$R$ [Mpc] ( $\tau_{54.4 \text{ eV}}^{\text{HeII}} \sim 1$ )	$\frac{\Delta}{\tau_{54.4 \text{ eV}}^{\text{HeII}}}$ ( $\tau_{54.4 \text{ eV}}^{\text{HeII}} \sim 1$ )	$\frac{\Delta T}{\tau_{54.4 \text{ eV}}^{\text{HeII}}}$ [K] ( $\tau_{54.4 \text{ eV}}^{\text{HeII}} \sim 1$ )	$\frac{\Gamma_{\text{HeII}}}{\Gamma_{\text{HeII}}^{\text{OT}}}$ ( $\tau_{54.4 \text{ eV}}^{\text{HeII}} \sim 1$ )	$\frac{\langle E \rangle_{\text{HeII}}}{\langle E \rangle_{\text{HeII}}^{\text{OT}}}$ ( $\tau_{54.4 \text{ eV}}^{\text{HeII}} \sim 1$ )
Fiducial, Fig. 4	6200	22.9	24.5	5.1	7900	0.66	1.21
$\alpha_s = 0.5$ , Fig. 4	10700	39.5	37.7	46.0	24200	0.25	2.14
$\alpha_s = 2.5$ , Fig. 4	4600	17.0	0.8	32.0	10900	0.94	1.03
Fiducial, Fig. 5	5400	19.9	33.5	0.2	5200	0.65	1.22
$L_B = 10^{13} L_\odot$ , Fig. 5	6300	23.3	71.4	4.7	7400	0.47	1.42
$L_B = 10^{11} L_\odot$ , Fig. 5	21100	77.9	0.8	222.4	43100	0.09	3.16

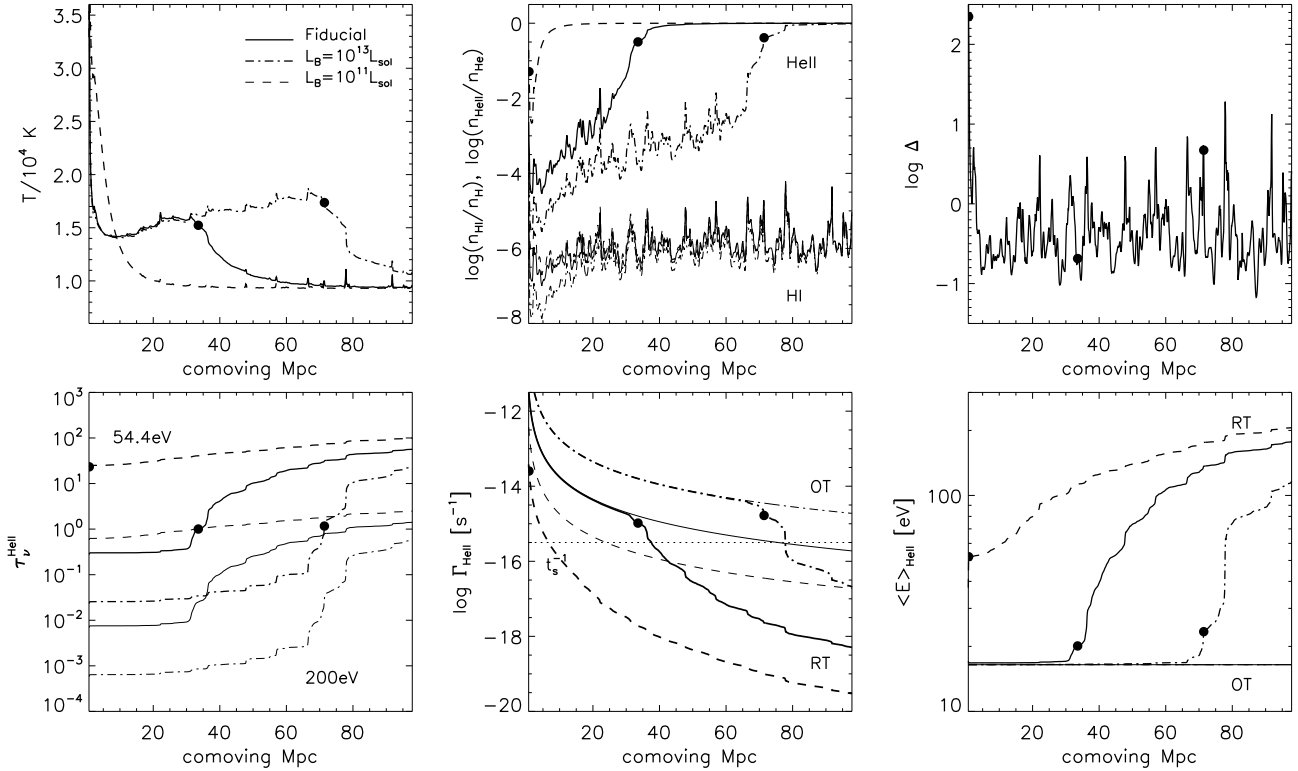


**Figure 5.** As for Fig. 4, except the EUV spectral index is now fixed at  $\alpha_s = 1.5$  and three different quasar luminosities are instead adopted: the fiducial model with  $L_B = 10^{12} L_\odot$  (solid curves),  $L_B = 10^{13} L_\odot$  (dash-dotted curves) and  $L_B = 10^{11} L_\odot$  (dashed curves). Note the IGM density distribution along this line-of-sight differs from Fig. 4.

temperatures of the reionised IGM ( $f_{\text{HeII}} < 0.1$ ) are  $\langle T \rangle = (20\,700, 16\,200, 14\,600)$  K for  $\alpha_s = (0.5, 1.5, 2.5)$ . For an initial temperature of  $T = 10^4$  K, this implies  $\langle \Delta T \rangle \simeq (10\,700, 6\,200, 4\,600)$  K, again consistent with the simple analytical estimates for  $\Delta T$  in Fig. 1. From eq. (7), these temperature boosts imply  $\langle E \rangle_{\text{HeII}} \simeq (40, 23, 17)$  eV, corresponding to (1.8, 1.5, 1.4) times  $\langle E \rangle_{\text{HeII}}$  evaluated in the optically thin limit. Excluding the biased regions within 5 Mpc of the quasar yields similar values;  $\langle \Delta T \rangle = (10\,800, 5\,900, 3\,900)$  K. Thus on average, most of the photo-heating over the quasar lifetime is achieved by the moderately filtered radiation close to the leading edge of the He III ionisation front. For comparison to other estimates, when neglecting re-emission from the IGM the updated calculations of Haardt & Madau (1996) indicate that  $\langle E \rangle_{\text{HeII}} = 24.9$  eV for  $\alpha_s = 1.57$  within a quasar dominated UV background model (F. Haardt, private communication). This is in good agreement with our results. Note, however, that including He III recombination emission lowers the average energy per photo-ionisation, such that  $\langle E \rangle_{\text{HeII}} = 17.5$  eV. This suggests that significant He III recombination emission may lower the expected IGM temperature boost even further by increasing the number of soft He II ionising photons.

In Fig. 5, the results for the fiducial quasar model along a different line-of-sight are compared to two further models with  $L_B = 10^{11} L_\odot$  (dashed curves) and  $L_B = 10^{13} L_\odot$  (dot-dashed curves). The IGM temperature again increases within  $\sim 5$  Mpc of the quasar in all models. However, in the

case of the  $L_B = 10^{11} L_\odot$  quasar, there is a significant temperature boost over a region  $R \sim 10$  Mpc. At first this may seem counter-intuitive; from the argument presented in §3.2, one might naively expect a faint ionising source to produce less heating due to longer photo-ionisation timescales. However, in this instance, the faint quasar has not had enough time to overcome the recombinations in its host halo, and as a result the radiation has been persistently filtered and hardened ( $\langle E \rangle_{\text{HeII}} \sim 38$  eV). This effect is relatively common in our simulated lines-of-sight for  $L_B = 10^{11} L_\odot$ . Note, however, this effect will be less prominent or even absent if all the He II within  $\sim 5$  Mpc of the quasar host halo has been previously photo-ionised or is instead shock-heated and hence collisionally ionised.

In comparison to the line-of-sight in Fig. 4, the IGM density distribution in Fig. 5 is also less dense on average. This results in slightly less spectral hardening close to the quasar. As a consequence, the fiducial model in Fig. 5 exhibits lower temperatures, with a maximum of 16 500 K at  $R = 22$  Mpc, while the  $L_B = 10^{13} L_\odot$  model has a maximum of  $T = 18\,700$  K at  $R = 67$  Mpc. The average temperatures in regions with  $f_{\text{HeII}} < 0.1$  are  $\langle T \rangle = (16\,300, 15\,400, 31\,100)$  K for  $L_B = (10^{13}, 10^{12}, 10^{11}) L_\odot$ . As before, this implies that the average excess energy per He II photo-ionisation is  $\langle E \rangle_{\text{HeII}} \simeq (23, 20, 78)$  eV, corresponding to (1.5, 1.3, 5.0) times  $\langle E \rangle_{\text{HeII}}$  evaluated in the optically thin limit. Again, the first two values are consistent with most of the photo-heating being due to only modestly

hardened radiation, whereas the latter model results in very large temperature boosts close to the quasar. Excluding the biased regions with 5 Mpc, the average temperatures are instead  $\langle T \rangle = (16\ 200, 15\ 100)$  K for  $L_B = (10^{13}, 10^{12})L_\odot$ ; there are no regions with  $f_{\text{HeII}} < 0.1$  at  $R > 5$  Mpc in the  $L_B = 10^{11}L_\odot$  line-of-sight.

We note briefly that observations of the H I and He II Ly $\alpha$  forest are another useful diagnostic of He II reionisation. Large fluctuations are observed in the measured column density ratio,  $\eta = N_{\text{HeII}}/N_{\text{HI}}$  (Zheng et al. 2004; Shull et al. 2004; Fechner et al. 2006). The average value of  $\eta$  also increases towards higher redshifts. Direct measurements of the softness parameter,  $S = \Gamma_{\text{HI}}/\Gamma_{\text{HeII}} \simeq 2.4\eta$ , give  $S = (139_{-67}^{+99}, 196_{-97}^{+170}, 301_{-151}^{+576})$  at  $z = (2.1, 2.4, 2.8)$  (Bolton et al. 2006). The large error bars are due to the very uncertain He II effective optical depth measured from the He II Ly $\alpha$  forest data. Our simulations are not able to follow  $\eta$ -fluctuations during He II reionisation in detail, since this requires a detailed treatment of the spatial distribution of ionising sources as well as radiative transfer (see *e.g.* Bolton et al. 2006; Paschos et al. 2007; Furlanetto 2008). However, we may still estimate the average softness parameter in our simulations along the line-of-sight from a single quasar. In regions with  $f_{\text{HeII}} < 0.1$ , this yields  $S = (52, 153, 338)$  for the lines-of-sight with  $\alpha_s = (0.5, 1.5, 2.5)$  in Fig. 4 and  $S = (131, 237, 698)$  for  $L_B = (10^{13}, 10^{12}, 10^{11})L_\odot$  in Fig. 5. These values are broadly consistent with the observational constraints, aside from the model with  $\alpha_s = 0.5$  which produces a spectrum which is too hard, indicating that this model may be somewhat extreme.

We have only shown the details for six of our line-of-sight radiative transfer calculations here, although these are quite typical examples from our large sample. The results from all the simulations will in any case be summarised in the next section. It is nevertheless clear from these examples that variations in quasar luminosities, lifetimes, and intrinsic spectra, as well as the intervening IGM density distribution, will result in a great deal of variation in the thermal and ionisation state of the IGM on small scales. Such detailed behaviour cannot be adequately captured by analytical or semi-analytical arguments. They do, however, confirm that our general expectations hold. For typical quasar luminosities and spectra at  $z \sim 3$ , temperature boosts during He II reionisation in excess of  $\sim 10^4$  K are unlikely to occur rapidly ( $\Delta z \lesssim 0.1 - 0.2$ ) over the entire IGM. Although large temperatures are indeed possible, these are most likely to occur either around very hard sources, or in highly overdense regions of the IGM. Furthermore, the hardest photons tend to be preferentially deposited in the densest clumps in the simulations, as is evidenced by the larger temperatures associated with these regions. Most of the low density IGM is reionised by the more numerous soft photons, leading to temperature boosts in the range of  $\Delta T = 5\ 000 - 10\ 000$  K for  $\alpha_s = 1.5$ . Note that in all instances, there is no strong photo-heating wherever  $\Gamma_{\text{HeII}} \ll t_s^{-1}$ .

## 7 THE IGM TEMPERATURE-DENSITY RELATION

There is some recent evidence to suggest that the IGM temperature-density relation may be substantially more complex than is usually assumed around  $z \simeq 3$ . Becker et al. (2007) and Bolton et al. (2008) have independently noted that the flux distribution of the Ly $\alpha$  forest is well reproduced by a model where the voids in the IGM are significantly hotter than expected, perhaps due to radiative transfer effects during He II reionisation which invert ( $\gamma < 1$ ) the IGM temperature-density relation. Complementary to this, Furlanetto & Oh (2008a) pointed out that the inhomogeneous distribution of He II ionising sources will also complicate the IGM temperature-density relation; voids are generally photo-ionised and heated last and are thus hotter towards the end stages of He II reionisation. Glezer et al. (2005) also demonstrated that the inhomogeneous nature of He II reionisation will blur the IGM temperature-density relation. We cannot address the three dimensional effects discussed in these latter studies with our radiative transfer simulations. However, we can quantify the impact filtering by the IGM will have on the IGM temperature-density relation.

Contour plots of the temperature-density planes for all nine sets of our radiative transfer simulations are displayed in Fig. 6. Each panel shows the results for 30 different lines-of-sight. In all panels, the annotated arrows indicate the temperature of the IGM for all gas at mean density with  $f_{\text{HeII}} < 0.1$  (upper arrows) and  $f_{\text{HeII}} > 0.9$  (lower arrows). The dotted lines represent the initial temperature-density relation adopted in the models. Regions with  $T \lesssim 10^4$  K are associated with He II which has not yet been significantly photo-ionised and heated.

The upper row in Fig. 6 displays, from left to right, the temperature-density plane for the fiducial quasar model, the hard quasar model ( $\alpha_s = 0.5$ ) and the soft model ( $\alpha_s = 2.5$ ). Again note the quasar models are normalised to have the same rest frame B-band luminosity, such that  $\dot{N}(\alpha_s = 0.5)/\dot{N}(\alpha_s = 1.5) \simeq 14$  and  $\dot{N}(\alpha_s = 2.5)/\dot{N}(\alpha_s = 1.5) \simeq 1/8$ . The largest temperatures are associated with the hard quasar model, where additionally the most He II has been photo-ionised and heated. The middle row, from left to right, displays the models with  $L_B = 10^{13}L_\odot$ ,  $L_B = 10^{11}L_\odot$  and  $t_s = 10^7$  yrs. Note that the  $L_B = 10^{11}L_\odot$  temperature-density plane exhibits the highest temperatures around mean density. This is due to photo-heating of the He II close to the quasar by intense but highly filtered radiation, as discussed in the previous section. Lastly, the lower row displays the same quasar models shown in the upper row, but now the IGM initially follows a tight power-law temperature density relation,  $T = T_0\Delta^{\gamma-1}$  for  $\Delta \leq 10$  and  $T = T_010^{\gamma-1}$  for  $\Delta > 10$ , where  $T_0 = 10^4$  K and  $\gamma = 1.3$ . The temperature-density relation in an optically thin IGM is expected to slowly asymptote to a power-law with  $\gamma \sim 1.6$  following H I reionisation (Hui & Gnedin 1997). This changes the *absolute* temperature of the underdense material in the IGM following He II reionisation, although the temperature boost at all densities remains similar to the isothermal case. Thus, the IGM temperature-density relation prior to He II reionisation clearly impacts its post-reionisation form, although again note that the heat

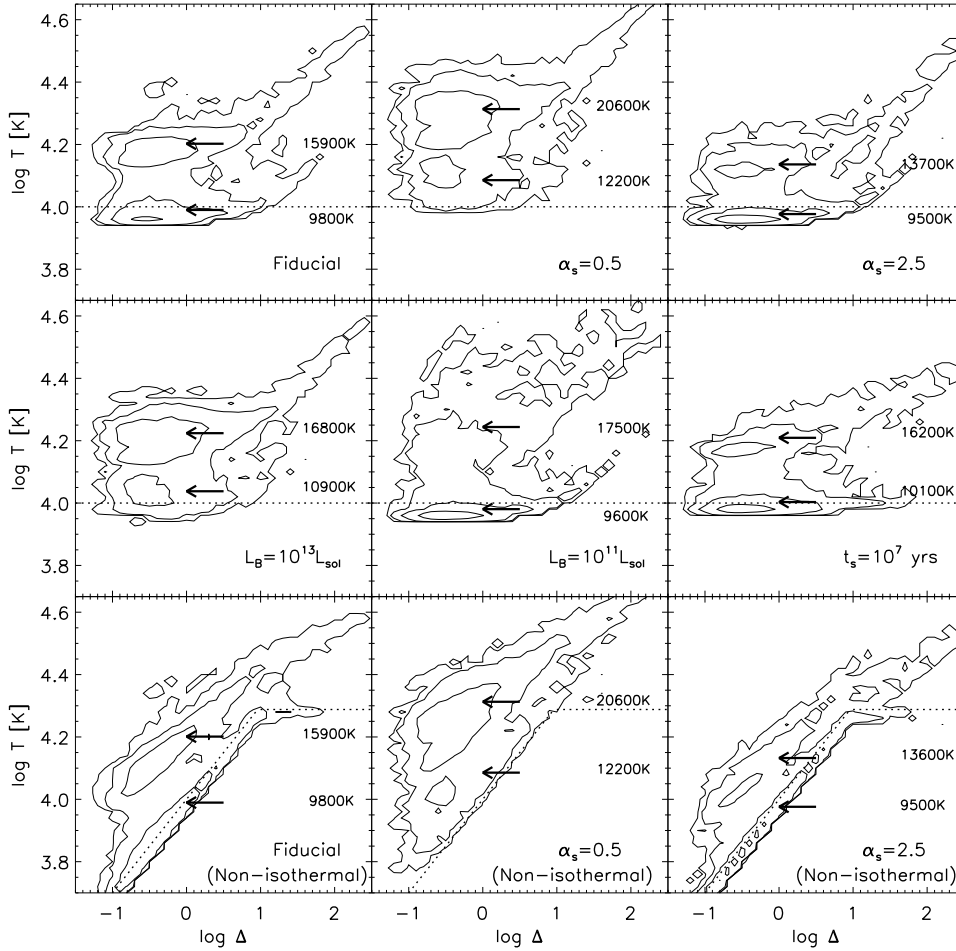


**Figure 6.** Contour plots of the volume weighted temperature-density plane at  $z = 3$  in nine different models of He II reionisation by quasars. Each panel shows the data from 30 different lines-of-sight through the IGM. The number density of the data points increases by an order of magnitude within successive contour levels. The two annotated arrows in each panel indicate the temperature of the IGM at mean density for regions with  $f_{\text{HeII}} < 0.1$  (upper arrows) and  $f_{\text{HeII}} > 0.9$  (lower arrows). In all panels, the IGM is initially in photo-ionisation equilibrium with the UVB specified by eq. (27). Regions with  $T \lesssim 10^4$  K are associated with He II which has not yet been significantly photo-ionised and heated. *Top row:* From left to right, the temperature-density plane for the fiducial quasar model ( $L_B = 10^{12} L_\odot$ ,  $\alpha_s = 1.5$ ,  $t_s = 10^8$  yrs) and models with harder ( $\alpha_s = 0.5$ ) and softer ( $\alpha_s = 2.5$ ) intrinsic spectra. *Middle row:* From left to right, the temperature-density plane for the quasar models with  $L_B = 10^{13} L_\odot$ ,  $L_B = 10^{11} L_\odot$  and  $t_s = 10^7$  yrs. The IGM temperature in all panels in the upper and middle rows is initially isothermal with  $T = 10^4$  K. *Bottom row:* As for the top row, except the temperature of the IGM initially follows a power law temperature density relation:  $T = T_0 \Delta^{\gamma-1}$  for  $\Delta \leq 10$ , with  $T = T_0 10^{\gamma-1}$  for  $\Delta > 10$ . We assume  $T_0 = 10^4$  K and  $\gamma = 1.3$ . The initial IGM temperature-density relations are represented by the dotted lines in all panels.

input into the IGM remains consistent with the analytical arguments presented earlier.

The average temperatures measured at four different densities,  $\log \Delta = (-1, 0, 1, 2)$ , in each of the models are summarised in Table 2. The largest temperature boosts occur in the densest regions in the simulations and are substantially higher than those expected in the optically thin limit as discussed in § 4. This suggests the hardest photons are preferentially deposited in these regions over the lifetime of the quasars. However, at mean density and below, the temperature boosts are much closer to the optically thin values, and only modest temperature boosts are achieved. In all panels there is also considerable scatter in the temperature-density plane. This is very different from the tight, power-law temperature-density relation expected for an optically

thin IGM (*e.g.* Hui & Gnedin 1997; Valageas et al. 2002). A similar result was noted by Bolton et al. (2004) following H I reionisation, who found that the temperature-density relation may even be inverted ( $\gamma < 1$ ). However, this was for a single line-of-sight only and thus not necessarily representative of the IGM as a whole. Tittley & Meiksin (2007) also found that radiative transfer effects can alter the temperature-density relation of the IGM, and will furthermore depend on the types of sources responsible for reionisation. On the other hand, using three dimensional radiative transfer simulations of He II reionisation, Paschos et al. (2007) found the IGM temperature-density relation is not inverted, although the IGM temperature is still increased by around a factor of two at mean density. However, the necessarily approximate frequency integration scheme they

**Table 2.** The average temperature boost in the IGM due to He II photo-heating measured from each group of simulations displayed in Fig. 6. The temperature boosts are computed at four different densities,  $\log \Delta = (-1, 0, 1, 2)$ , and correspond to the temperatures in regions with  $f_{\text{HeII}} < 0.1$  only. For comparison, the final column lists the expected temperature boost in the optically thin limit computed using eq. (7).

Model	$\langle \Delta T \rangle$ [K] ( $\log \Delta = -1$ )	$\langle \Delta T \rangle$ [K] ( $\log \Delta = 0$ )	$\langle \Delta T \rangle$ [K] ( $\log \Delta = 1$ )	$\langle \Delta T \rangle$ [K] ( $\log \Delta = 2$ )	$\Delta T_{\text{OT}}$ [K]
Fiducial	5300	5900	9400	21300	4200
$\alpha_s = 0.5$	10400	10600	14900	30100	5900
$\alpha_s = 2.5$	3500	3700	4600	16100	3300
$L_B = 10^{13} L_\odot$	6600	6800	9500	21400	4200
$L_B = 10^{11} L_\odot$	5300	7500	15700	26700	4200
$t_s = 10^7$ yrs	5300	6200	9100	14400	4200
Fiducial (non-isothermal)	5900	5900	7200	15600	4200
$\alpha_s = 0.5$ (non-isothermal)	11000	10600	12800	24800	5900
$\alpha_s = 2.5$ (non-isothermal)	4000	3600	2000	9400	3300

use in order to run such a detailed simulation may not model the reprocessing of the ionising radiation field precisely.

It is nevertheless clear from Fig. 6 that although voids in the IGM are significantly heated during He II reionisation, a well-defined, inverted temperature-density relation appears difficult to achieve with line-of-sight radiative transfer alone (see also McQuinn et al. 2008). Empirical interpretations of the Ly $\alpha$  forest data seem to indicate such an inversion, but (as noted by Bolton et al. 2008) the mild inversion apparently required in such studies may simply mimic a more complex relationship between temperature and density in the IGM. Following He II reionisation, the temperature scatter in each model increases considerably, and over the entire IGM it may be larger still. Differences in quasar properties and the local density distribution of the IGM, as well as the thermal state of the IGM immediately prior to He II reionisation, could enhance the overall scatter. The simulations also suggest the extent to which He II reionisation has progressed will have an important effect on the IGM temperature-density relation. Prior to the completion of He II reionisation, a two-phase medium with hot He III regions and cooler regions of He II should develop, leading to large fluctuations in the IGM temperature. Note that a correct treatment of the timing of He II reionisation at different densities is also required to model this properly (Furlanetto & Oh 2008a), and the reionisation of partially recombined fossil He III regions will complicate the temperature-density relation yet further. On the other hand, studies using wavelets (Theuns et al. 2002b) have failed to detect spatial fluctuations in the IGM temperature on small scales at  $z \simeq 3$ . However, these studies are implicitly predicated on fairly large (around a factor of two) temperature boosts; more modest boosts over small scales may be hard to extract from the data.

## 8 CONCLUSIONS AND DISCUSSION

In this work we have performed a detailed analysis of the photo-heating of the IGM during He II reionisation using a combination of analytical arguments and numerical radiative transfer models. Our aim was to critically examine the physical processes involved in modelling the fate of hard,

He II ionising photons in the IGM and their impact on the thermal evolution of the IGM. The main results of this work are as follows.

(i) Filtering through the IGM weakens as well as hardens ionising radiation (Abel & Haehnelt 1999; Bolton et al. 2004). However, significant photo-heating of the IGM during He II reionisation can only occur over timescales comparable to or shorter than the local He II photo-ionisation timescale,  $t_{\text{ion}} = \Gamma_{\text{HeII}}^{-1}$ , irrespective of the mean excess energy per He II photo-ionisation,  $\langle E \rangle_{\text{HeII}}$ . Consequently, this limits the temperature boost,  $\Delta T$ , attainable over a given timescale within a fixed volume of the IGM. For an  $L_*$  quasar at  $z = 3$  with a typical EUV spectra index of  $\alpha_s = 1.5$  and a lifetime  $t_s = 10^8$  yrs,  $\Delta T$  will not exceed  $10^4$  K at distances  $R > 40$  Mpc from the quasar, and will furthermore only do so at  $R < 40$  Mpc if the softer photons near the He II ionisation edge do not contribute towards photo-ionisation. For an average separation between  $L_*$  quasars of  $\sim 100$  Mpc, this implies a global temperature boost of  $\Delta T \gtrsim 10^4$  K over  $\Delta z = 0.1 - 0.2$  is difficult to achieve unless quasars with much harder EUV spectra are common.

(ii) Hard photons are preferentially absorbed in the densest regions of the IGM where the largest temperature boosts will thus occur. However, current constraints on the IGM temperature based on observations of the low column density Ly $\alpha$  forest (Schaye et al. 2000; Ricotti et al. 2000; McDonald et al. 2001) are mainly sensitive to densities close to the cosmic mean or below (Schaye 2001). The fate of hard photons and expected heating rates thus depends on the relative abundance of high column density  $N_{\text{HeII}}$  absorbers: if most of the heat is deposited in dense systems, we have no way of inferring this from the Ly $\alpha$  forest. Unfortunately, the abundance of such systems is rather model-dependent, and varies with the unknown radiation field  $\Gamma_{\text{HeII}}$  during reionisation and the correspondence between physical density  $n_{\text{H}}$  and observed column densities  $N_{\text{HI}}$ . This translates into considerable uncertainties in the photo-heating rates and the resulting IGM temperature boost. A plausible range of values, given model uncertainties, is  $\Delta T \approx 7,000 - 15,000$  K, somewhat intermediate between the optical thin and thick values of  $\Delta T \approx 4,000$  K and  $\Delta T \approx 30,000$  K respectively, for a  $J_\nu \propto \nu^{-1.5}$  unprocessed source spectrum.

(iii) Even though the mean separation between He II Lyman limit systems is comparable to the expected size of He III regions around  $L_*$  quasars, most of the IGM could potentially still be ionised primarily by soft photons, at least if quasars are randomly distributed. If this were the case, the average amount of heating over the entire IGM would be relatively modest. In general, only unusual regions that are far from the ionising sources will be exposed to a highly-filtered spectrum for a long enough period to heat substantially. This can only happen toward the end of He II reionisation, because the photo-ionisation timescale is so long for such heavily filtered spectra.

(iv) The reheating of partially recombined fossil He III regions is unlikely to substantially increase the IGM temperature beyond that achieved during the first round of He II reionisation. In general, recombination timescales in these fossil regions typically exceed cooling timescales and the average time lag between ionisations by successive generations of quasars. The net heating is therefore not increased.

(v) We run a detailed set of 270 line-of-sight radiative transfer simulations using a variety of initial conditions to confirm these analytic predictions. We further demonstrate that the filtering of ionising radiation through the IGM will produce a rich thermal structure. This is likely to be further complicated by the inhomogeneous distribution of the ionising sources and the typically short lifetimes of quasars (Furlanetto & Oh 2008a). This complex, multi-valued temperature-density relation may help to resolve discrepancies between optically thin hydrodynamical simulations of the Ly $\alpha$  forest and recent detailed observations (Bolton et al. 2008)

How do these conclusions compare to the current observational constraints on the IGM thermal state at  $z = 3$ ? In the case of the magnitude of the IGM temperature boost, measurements of the Doppler widths of absorption lines in the Ly $\alpha$  forest currently offer the best constraints. The data of Schaye et al. (2000) are consistent with a relatively sharp ( $\Delta z \simeq 0.2$ ), large ( $\Delta T > 10^4$  K) temperature jump occurring around  $z = 3.3$  at densities around the cosmic mean. However, the error bars on these measurements are still large, and a more gradual, moderate temperature boost, as suggested by this work, is also consistent with the data. Similarly, the results of Ricotti et al. (2000) are also consistent with a significant and sudden temperature boost at  $z \sim 3$ , although large statistical errors again leave a more gentle thermal evolution possible. On the other hand, McDonald et al. (2001) find no evidence for a rapid boost in the IGM temperature at  $z \sim 3$ . Their constraints, corrected to correspond to measurements at mean density, at most allow only for a modest evolution in the IGM temperature ( $\Delta T \sim 4\,000$  K between  $z = 2 - 4$ ), and are also consistent with no temperature evolution at all. A detailed analysis of a large set of high resolution Ly $\alpha$  forest spectra, perhaps using alternative temperature sensitive statistics, is necessary to obtain improved constraints on the thermal state of the IGM at these redshifts.

Another intriguing result which may indirectly favour a rapid heat input scenario, somewhat at odds with the results presented here, is the evidence for a sharp dip ( $\Delta z = 0.2$ ) of around 10 per cent in the effective optical

depth of the Ly $\alpha$  forest at  $z = 3.2$  (Bernardi et al. 2003; Faucher-Giguere et al. 2008). Theuns et al. (2002a) used hydrodynamical simulations to interpret this feature as being due to a sudden increase in the IGM temperature at  $z \simeq 3.2$ , such that  $\Delta T \sim 10^4$  K. However, our results suggest that it is unlikely this transition could occur globally over such a short period. Alternatively, this feature may instead be due to a rapid change in the hydrogen photo-ionisation rate at  $z = 3.2$ , although again there is no current evidence to suggest this may be the case. Further investigation into this feature using detailed hydrodynamical simulations of the IGM is thus desirable.

Our results therefore suggest a general picture for the thermal evolution of the IGM during He II reionisation by quasars where: (i) the temperature boost during He II reionisation is significantly uncertain, and could be considerably less than has been commonly assumed in the optically thick heating limit, (ii) any such temperature boost must be achieved over a timescale longer than  $\Delta z > 0.1 - 0.2$  and (iii) the resulting temperature-density relation in the IGM will be much more complex than the tight, power-law temperature density relation expected in an optically thin IGM. Finally, we note that these results will not apply if the He II in the IGM is predominantly reionised by sources other than quasars. If the He II in the IGM is reionised early on by stellar sources, high redshift X-rays, thermal emission from shocked gas or some other, as yet unidentified source, then the thermal evolution of the IGM during He II reionisation may be rather different.

## ACKNOWLEDGEMENTS

We thank George Becker, Adam Lidz, Martin Haehnelt and Matteo Viel for helpful discussions during the course of this work, and the anonymous referee for a helpful report which improved this manuscript. We also thank Francesco Haardt for sharing his numerical results with us, and we are especially grateful to Matthew McQuinn for drawing our attention to several errors in the original manuscript. The hydrodynamical simulation used in this work was run using the SGI Altix 4700 supercomputer COSMOS at the Department of Applied Mathematics and Theoretical Physics in Cambridge. COSMOS is a UK-CCC facility which is sponsored by SGI, Intel, HECCE and STFC. This research was also supported in part by the National Science Foundation under Grant No. PHY05-51164 (JSB, through the MPA/KITP postdoctoral exchange programme), AST-0407084 (SPO) and AST-0829737 (SRF), and NASA grant NNG06GH95G (SPO). JSB thanks the staff at the Kavli Institute for Theoretical Physics, Santa Barbara, for their hospitality during the early stages of this work.

## REFERENCES

- Abel, T. & Haehnelt, M. G. 1999, *ApJ*, 520, L13
- Abel, T., Norman, M. L., & Madau, P. 1999, *ApJ*, 523, L66
- Becker, G. D., Rauch, M., & Sargent, W. L. W. 2007, *ApJ*, 662, 72
- Bernardi, M. et al. 2003, *AJ*, 125, 32

- Bolton, J., Meiksin, A., & White, M. 2004, *MNRAS*, 348, L43
- Bolton, J. S. & Haehnelt, M. G. 2007a, *MNRAS*, 374, 493
- Bolton, J. S. & Haehnelt, M. G. 2007b, *MNRAS*, 382, 325
- Bolton, J. S., Haehnelt, M. G., Viel, M., & Carswell, R. F. 2006, *MNRAS*, 366, 1378
- Bolton, J. S., Haehnelt, M. G., Viel, M., & Springel, V. 2005, *MNRAS*, 357, 1178
- Bolton, J. S., Viel, M., Kim, T.-S., Haehnelt, M. G., & Carswell, R. F. 2008, *MNRAS*, 386, 1131
- Davidson, A. F., Kriss, G. A., & Wei, Z. 1996, *Nature*, 380, 47
- Dijkstra, M., Haiman, Z., & Loeb, A. 2004, *ApJ*, 613, 646
- Dunkley, J. et al. 2009, *ApJS*, 180, 306
- Efstathiou, G. 1992, *MNRAS*, 256, 43
- Fan, X., Narayanan, V. K., Strauss, M. A., White, R. L., Becker, R. H., Pentericci, L., & Rix, H.-W. 2002, *AJ*, 123, 1247
- Fan X. et al., 2006, *AJ*, 132, 117
- Fardal, M. A., Giroux, M. L., & Shull, J. M. 1998, *AJ*, 115, 2206
- Faucher-Giguere, C.-A., Prochaska, J. X., Lidz, A., Hernquist, L., & Zaldarriaga, M. 2008, *ApJ*, 681, 831
- Fechner, C. et al. 2006, *A&A*, 455, 91
- Furlanetto, S. R. 2008, *ApJ* submitted, arXiv:0812.3411
- Furlanetto, S., Haiman, Z., & Oh, S. P. 2008, *ApJ*, 686, 25
- Furlanetto, S. & Oh, S. P. 2008a, *ApJ*, 682, 14
- Furlanetto, S. & Oh, S. P. 2008b, *ApJ*, 681, 1
- Furlanetto, S. R. & Oh, S. P. 2005, *MNRAS*, 363, 1031
- Giroux, M. L. & Shapiro, P. R. 1996, *ApJS*, 102, 191
- Gleser, L., Nusser, A., Benson, A. J., Ohno, H., & Sugiyama, N. 2005, *MNRAS*, 361, 1399
- Haardt, F. & Madau, P. 1996, *ApJ*, 461, 20
- Hansen, M. & Oh, S. P. 2006, *MNRAS*, 367, 979
- Heap, S. R., Williger, G. M., Smette, A., Hubeny, I., Sahu, M. S., Jenkins, E. B., Tripp, T. M., & Winkler, J. N. 2000, *ApJ*, 534, 69
- Hopkins, P. F., Hernquist, L., Cox, T. J., Di Matteo, T., Martini, P., Robertson, B., & Springel, V. 2005a, *ApJ*, 630, 705
- Hopkins, P. F., Hernquist, L., Martini, P., Cox, T. J., Robertson, B., Di Matteo, T., & Springel, V. 2005b, *ApJ*, 625, L71
- Hopkins, P. F., Richards, G. T., & Hernquist, L. 2007, *ApJ*, 654, 731
- Hui, L. & Gnedin, N. Y. 1997, *MNRAS*, 292, 27
- Hui, L. & Haiman, Z. 2003, *ApJ*, 596, 9
- Inoue, A. K. & Kamaya, H. 2003, *MNRAS*, 341, L7
- Jakobsen, P., Boksenberg, A., Deharveng, J. M., Greenfield, P., Jedrzejewski, R., & Paresce, F. 1994, *Nature*, 370, 35
- Jiang, L. et al. 2008, *AJ*, 135, 1057
- Katz, N., Weinberg, D. H., & Hernquist, L. 1996, *ApJS*, 105, 19
- Kim, T.-S., Carswell, R. F., Cristiani, S., D'Odorico, S., & Giallongo, E. 2002, *MNRAS*, 335, 555
- Lidz, A., Hopkins, P. F., Cox, T. J., Hernquist, L., & Robertson, B. 2006, *ApJ*, 641, 41
- Madau, P., Haardt, F., & Rees, M. J. 1999, *ApJ*, 514, 648
- Maio, U., Dolag, K., Ciardi, B., & Tornatore, L. 2007, *MNRAS*, 379, 963
- Martini, P. 2004, in *Coevolution of Black Holes and Galaxies*, Ho, L. C. ed., p.169
- Maselli, A. & Ferrara, A. 2005, *MNRAS*, 364, 1429
- McDonald, P., Miralda-Escudé, J., Rauch, M., Sargent, W. L. W., Barlow, T. A., & Cen, R. 2001, *ApJ*, 562, 52
- McDonald, P. et al. 2005, *ApJ*, 635, 761
- McQuinn, M., Lidz, A., Zaldarriaga, M., Hernquist, L., Hopkins, P. F., Dutta, S., & Faucher-Giguere, C.-A., 2008, *ApJin* press, arXiv:0807.2799
- Meiksin, A. 2005, *MNRAS*, 356, 596
- Miniati, F., Ferrara, A., White, S. D. M., & Bianchi, S. 2004, *MNRAS*, 348, 964
- Miralda-Escudé, J., & Ostriker, J. P. 1992, *ApJ*, 392, 15
- Miralda-Escudé, J., Haehnelt, M., & Rees, M. J. 2000, *ApJ*, 530, 1
- Miralda-Escudé, J. & Rees, M. J. 1994, *MNRAS*, 266, 343
- Oh, S. P. 2001, *ApJ*, 553, 499
- Oh, S. P., Nollett, K. M., Madau, P., & Wasserburg, G. J. 2001, *ApJ*, 562, L1
- Olive, K. A. & Skillman, E. D. 2004, *ApJ*, 617, 29
- Osterbrock, D. E. 1989, *Astrophysics of Gaseous Nebulae and Active Galactic Nuclei*, University Science Books, Mill Valley, CA
- Paresce, F., McKee, C. F., & Bowyer, S. 1980, *ApJ*, 240, 387
- Paschos, P., Norman, M. L., Bordner, J. O., & Harkness, R. 2007, preprint, arXiv:0711.1904
- Pettini, M. 2004, in *Cosmochemistry. The melting pot of the elements*, ed. C. Esteban, R. García López, A. Herrero, & F. Sánchez, 257–298
- Reimers, D., Fechner, C., Hagen, H.-J., Jakobsen, P., Tytler, D., & Kirkman, D. 2005, *A&A*, 442, 63
- Ricotti, M., Gnedin, N. Y., & Shull, J. M. 2000, *ApJ*, 534, 41
- Ricotti, M., Gnedin, N. Y., & Shull, J. M. 2002, *ApJ*, 575, 33
- Ricotti, M. & Ostriker, J. P. 2004, *MNRAS*, 352, 547
- Schaye, J. 2001, *ApJ*, 559, 507
- Schaye, J., Theuns, T., Rauch, M., Efstathiou, G., & Sargent, W. L. W. 2000, *MNRAS*, 318, 817
- Scott, J. E., Kriss, G. A., Brotherton, M., Green, R. F., Hutchings, J., Shull, J. M., & Zheng, W. 2004, *ApJ*, 615, 135
- Shapley, A. E., Steidel, C. C., Pettini, M., & Adelberger, K. L. 2003, *ApJ*, 588, 65
- Shen, Y. et al. 2007, *AJ*, 133, 2222
- Shull, J. M., Tumlinson, J., Giroux, M. L., Kriss, G. A., & Reimers, D. 2004, *ApJ*, 600, 570
- Smette, A., Heap, S. R., Williger, G. M., Tripp, T. M., Jenkins, E. B., & Songaila, A. 2002, *ApJ*, 564, 542
- Smith, B., Sigurdsson, S., & Abel, T. 2008, *MNRAS*, 385, 1443
- Sokasian, A., Abel, T., & Hernquist, L. 2002, *MNRAS*, 332, 601
- Songaila, A. 1998, *AJ*, 115, 2184
- Springel, V. 2005, *MNRAS*, 364, 1105
- Srbínovský, J. A. & Wyithe, J. S. B. 2007, *MNRAS*, 374, 627
- Telfer, R. C., Zheng, W., Kriss, G. A., & Davidson, A. F. 2002, *ApJ*, 565, 773
- Theuns, T. 2005, in *IAU Colloq. 199: Probing Galaxies through Quasar Absorption Lines*, Williams, P., Shu, C.-G. and Menard, B. eds., p.185

- Theuns, T., Bernardi, M., Frieman, J., Hewett, P., Schaye, J., Sheth, R. K., & Subbarao, M. 2002a, *ApJ*, 574, L111
- Theuns, T., Zaroubi, S., Kim, T.-S., Tzanavaris, P., & Carswell, R. F. 2002b, *MNRAS*, 332, 367
- Tittley, E. R. & Meiksin, A. 2007, *MNRAS*, 380, 1369
- Valageas, P., Schaeffer, R., & Silk, J. 2002, *A&A*, 388, 741
- Venkatesan, A., Giroux, M. L., & Shull, J. M. 2001, *ApJ*, 563, 1
- Venkatesan, A., Tumlinson, J., & Shull, J. M. 2003, *ApJ*, 584, 621
- Verner, D. A., Ferland, G. J., Korista, K. T., & Yakovlev, D. G. 1996, *ApJ*, 465, 487
- Vladilo, G., Centurión, M., D’Odorico, V., & Péroux, C. 2003, *A&A*, 402, 487
- Wiersma, R. P. C., Schaye, J., & Smith, B. D. 2009, *MNRAS*, 393, 99
- Zaldarriaga, M., Hui, L., & Tegmark, M. 2001, *ApJ*, 557, 519
- Zheng, W. et al. 2004, *ApJ*, 605, 631
- Zheng, W., Kriss, G. A., Telfer, R. C., Grimes, J. P., & Davidsen, A. F. 1997, *ApJ*, 475, 469
- Zuo, L. & Phinney, E. S. 1993, *ApJ*, 418, 28